[15] Funahashi T, Nakamura T, Shimomura I, Maeda K, Kuriyama H, Takahashi M, et al. Role of adipocytokines on the pathogenesis of atherosclerosis in visceral obesity. Intern Med 1999;38:202–6.
[16] Takahashi M, Arita Y, Yamagata K, Matsukawa Y, Okutomi K, Horie M, et al. Genomic structure and mutations in adipose-specific gene, adiponectin. Int J Obes Relat Metab Disord 2000;24:861–8.
[17] Pischon T, Girman CJ, Hotamisligil GS, Rifai N, Hu FB, Rimm EB. Plasma adiponectin levels and risk of myocardial infarction in men. Jama 2004;291:1730–7.
[18] Shibata R, Ouchi N, Ito M, Kihara S, Shiojima I, Pimentel DR, et al. Adiponectin-mediated modulation of hypertrophic signals in the heart. Nat Med 2004;10:1384–9.
[19] Maeda N, Shimomura I, Kishida K, Nishizawa H, Matsuda M, Nagaretani H, et al. Diet-induced insulin resistance in mice lacking adiponectin/ACRP30. Nat Med 2002;8:731–7.
[20] Sanada S, Node K, Minamino T, Takashima S, Ogai A, Asanuma H, et al. Long-acting Ca2+ blockers prevent myocardial remodeling induced by chronic NO inhibition in rats. Hypertension 2003;41: 963–7.
[21] Liao Y, Asakura M, Takashima S, Ogai A, Asano Y, Asanuma H, et al. Benidipine, a long-acting calcium channel blocker, inhibits cardiac remodeling in pressure-overloaded mice. Cardiovasc Res 2005;65: 879–88.
[22] Liao Y, Ishikura F, Beppu S, Asakura M, Takashima S, Asanuma H, et al. Echocardiographic assessment of LV hypertrophy and function in aortic-banded mice: necropsy validation. Am J Physiol Heart Circ Physiol 2002;282:H1703–8.
[23] Liao Y, Takashima S, Asano Y, Asakura M, Ogai A, Shintani Y, et al. Activation of adenosine A1 receptor attenuates cardiac hypertrophy and prevents heart failure in murine left ventricular pressure-overload model. Circ Res 2003;93:759–66.
[24] Liao Y, Asakura M, Takashima S, Ogai A, Asano Y, Shintani Y, et al. Celiprolol, a vasodilatory beta-blocker, inhibits pressure overload-induced cardiac hypertrophy and prevents the transition to heart failure via nitric oxide-dependent mechanisms in mice. Circulation 2004;110: 692–9.
[25] Roth DM, Swaney JS, Dalton ND, Gilpin EA, Ross Jr J. Impact of anesthesia on cardiac function during echocardiography in mice. Am J Physiol Heart Circ Physiol 2002;282:H2134–40.
[26] Tsuchida A, Yamauchi T, Ito Y, Hada Y, Maki T, Takekawa S, et al. Insulin/Foxo1 pathway regulates expression levels of adiponectin receptors and adiponectin sensitivity. J Biol Chem 2004;279:30817–22.
[27] Nakae J, Biggs III WH, Kitamura T, Cavenee WK, Wright CV, Arden KC, et al. Regulation of insulin action and pancreatic beta-cell function by mutated alleles of the gene encoding forkhead transcription factor Foxo1. Nat Genet 2002;32:245–53.
[28] Brunner EJ, Hemingway H, Walker BR, Page M, Clarke P, Juneja M, et al. Adrenocortical, autonomic, and inflammatory causes of the metabolic syndrome: nested case-control study. Circulation 2002;106: 2659–65.
[29] Prasad A, Quyyumi AA. Renin–angiotensin system and angiotensin receptor blockers in the metabolic syndrome. Circulation 2004;110: 1507–12.
[30] Malik S, Wong ND, Franklin SS, Kamath TV, L'Italien GJ, Pio JR, et al. Impact of the metabolic syndrome on mortality from coronary heart disease, cardiovascular disease, and all causes in United States adults. Circulation 2004;110:1245–50.
[31] Trevisan M, Liu J, Bahsas FB, Menotti A. Syndrome X and mortality: a population-based study. Risk factor and life expectancy research group. Am J Epidemiol 1998;148:958–66.
[32] Lakka HM, Laaksonen DE, Lakka TA, Niskanen LK, Kumpusalo E, Tuomilehto J, et al. The metabolic syndrome and total and cardiovascular disease mortality in middle-aged men. Jama 2002;288:2709–16.
[33] Chinali M, Devereux RB, Howard BV, Roman MJ, Bella JN, Liu JE, et al. Comparison of cardiac structure and function in American Indians with and without the metabolic syndrome (the Strong Heart Study). Am J Cardiol 2004;93:40–4.
[34] de Kreutzenberg SV, Avogaro A, Tiengo A, Del Prato S. Left ventricular mass in type 2 diabetes mellitus. A study employing a simple ECG index: the Cornell voltage. J Endocrinol Invest 2000;23: 139–44.
[35] Sundstrom J, Lind L, Nystrom N, Zethelius B, Andren B, Hales CN, et al. Left ventricular concentric remodeling rather than left ventricular hypertrophy is related to the insulin resistance syndrome in elderly men. Circulation 2000;101:2595–600.
[36] Paolisso G, Galderisi M, Tagliamonte MR, de Divitis M, Galzerano D, Petrocelli A, et al. Myocardial wall thickness and left ventricular geometry in hypertensives. Relationship with insulin. Am J Hypertens 1997;10:1250–6.
[37] Altarejos JY, Taniguchi M, Clanachan AS, Lopaschuk GD. Myocardial ischemia differentially regulates LKB1 and an alternate 5′-AMP-activated protein kinase kinase. J Biol Chem 2005;280:183–90.
[38] Kantor PF, Robertson MA, Coe JY, Lopaschuk GD. Volume overload hypertrophy of the newborn heart slows the maturation of enzymes involved in the regulation of fatty acid metabolism. J Am Coll Cardiol 1999;33:1724–34.
[39] Motoshima H, Wu X, Mahadev K, Goldstein BJ. Adiponectin suppresses proliferation and superoxide generation and enhances eNOS activity in endothelial cells treated with oxidized LDL. Biochem Biophys Res Commun 2004;315:264–71.
[40] Brakenhielm E, Veitonmaki N, Cao R, Kihara S, Matsuzawa Y, Zhivotovsky B, et al. Adiponectin-induced antiangiogenesis and antitumor activity involve caspase-mediated endothelial cell apoptosis. Proc Natl Acad Sci U S A 2004;101:2476–81.
[41] Fasshauer M, Klein J, Neumann S, Eszlinger M, Paschke R. Adiponectin gene expression is inhibited by beta-adrenergic stimulation via protein kinase A in 3T3-L1 adipocytes. FEBS Lett 2001; 507:142–6.
[42] Grundy SM, Brewer Jr HB, Cleeman JI, Smith Jr SC, Lenfant C. Definition of metabolic syndrome: report of the National Heart, Lung, and Blood Institute/American Heart Association conference on scientific issues related to definition. Circulation 2004;109:433–8.
[43] Li J, Hu X, Selvakumar P, Russell III RR, Cushman SW, Holman GD, et al. Role of the nitric oxide pathway in AMPK-mediated glucose uptake and GLUT4 translocation in heart muscle. Am J Physiol Endocrinol Metab 2004;287:E834–41.
[44] Chen ZP, Mitchelhill KI, Michell BJ, Stapleton D, Rodriguez-Crespo I, Witters LA, et al. AMP-activated protein kinase phosphorylation of endothelial NO synthase. FEBS Lett 1999;443:285–9.

Overexpression of Mitochondrial Peroxiredoxin-3 Prevents Left Ventricular Remodeling and Failure After Myocardial Infarction in Mice

Shouji Matsushima, MD; Tomomi Ide, MD, PhD; Mayumi Yamato, PhD; Hidenori Matsusaka, MD; Fumiyuki Hattori, PhD; Masaki Ikeuchi, MD; Toru Kubota, MD, PhD; Kenji Sunagawa, MD, PhD; Yasuhiro Hasegawa, PhD; Tatsuya Kurihara, PhD; Shinzo Oikawa, PhD; Shintaro Kinugawa, MD, PhD; Hiroyuki Tsutsui, MD, PhD

Background—Mitochondrial oxidative stress and damage play major roles in the development and progression of left ventricular (LV) remodeling and failure after myocardial infarction (MI). We hypothesized that overexpression of the mitochondrial antioxidant, peroxiredoxin-3 (Prx-3), could attenuate this deleterious process.

Methods and Results—We created MI in 12- to 16-week-old, male Prx-3–transgenic mice (TG+MI, n=37) and nontransgenic wild-type mice (WT+MI, n=39) by ligating the left coronary artery. Prx-3 protein levels were 1.8 times higher in the hearts from TG than WT mice, with no significant changes in other antioxidant enzymes. At 4 weeks after MI, LV thiobarbituric acid–reactive substances in the mitochondria were significantly lower in TG+MI than in WT+MI mice (mean±SEM, 1.5±0.2 vs 2.2±0.2 nmol/mg protein; n=8 each, $P<0.05$). LV cavity dilatation and dysfunction were attenuated in TG+MI compared with WT+MI mice, with no significant differences in infarct size (56±1% vs 55±1%; n=6 each, P=NS) and aortic pressure between groups. Mean LV end-diastolic pressures and lung weights in TG+MI mice were also larger than those in WT+sham-operated mice but smaller than those in WT+MI mice. Improvement in LV function in TG+MI mice was accompanied by a decrease in myocyte hypertrophy, interstitial fibrosis, and apoptosis in the noninfarcted LV. Mitochondrial DNA copy number and complex enzyme activities were significantly decreased in WT+MI mice, and this decrease was also ameliorated in TG+MI mice.

Conclusions—Overexpression of Prx-3 inhibited LV remodeling and failure after MI. Therapies designed to interfere with mitochondrial oxidative stress including the antioxidant Prx-3 might be beneficial in preventing cardiac failure. **(*Circulation*. 2006;113:1779-1786.)**

Key Words: antioxidants ■ free radicals ■ heart failure ■ myocardial infarction ■ remodeling

Experimental and clinical studies have demonstrated excessive generation of reactive oxygen species (ROS) in failing hearts.[1,2] Among the potential sources of ROS within the heart, mitochondrial electron transport produces superoxide anion ($\cdot O_2^-$) in this disease state.[3] Furthermore, increased ROS leads to mitochondrial DNA (mtDNA) damage and dysfunction.[4,5] Therefore, the intimate link between mitochondrial oxidative stress, mtDNA decline, and mitochondrial dysfunction plays an important role in the development and progression of left ventricular (LV) remodeling and failure that occur after myocardial infarction (MI).

Clinical Perspective p 1786

Peroxiredoxin-3 (Prx-3) is a mitochondrial antioxidant protein and member of the Prx family that can scavenge H_2O_2 in cooperation with thiol and peroxynitrite.[6] In mammals, 6 distinct Prx family members have been identified (Prx-1 through -6). Among the Prxs, Prx-3 is unique because it is localized specifically within the mitochondria.[7] Furthermore, in vivo transfer of the *Prx-3* gene protected neurons against cell death induced by oxidative stress.[8] These beneficial characteristics make Prx-3 an important candidate for therapy against LV failure after MI, in which ROS production has been demonstrated to be increased within the mitochondria.[1,4] Although several previous reports showed the beneficial effects of antioxidants on heart failure,[9,10] no study has ever been performed to specifically examine the protective role of Prx-3. To address these questions, we created transgenic (TG) mice containing the rat *Prx-3* gene. Rat Prx-3–TG mice and their wild-type (WT) littermates were randomized to receive

Received August 10, 2005; revision received January 26, 2006; accepted February 2, 2006.

From the Department of Cardiovascular Medicine, Graduate School of Medical Sciences (S.M., T.I., H.M., M.I., T.K., K.S.), and the Department of Redox Medicinal Science, Graduate School of Pharmaceutical Sciences (M.Y.), Kyushu University, Fukuoka; Biomedical Research Laboratories (F.H., Y.H., T.K., S.O.), Daiichi Suntory Pharma Co, Ltd, Osaka; and the Department of Cardiovascular Medicine (S.K., H.T.), Hokkaido University Graduate School of Medicine, Sapporo, Japan.

Correspondence to Hiroyuki Tsutsui, MD, PhD, Department of Cardiovascular Medicine, Hokkaido University Graduate School of Medicine, Kita-15, Nishi-7, Kita-ku, Sapporo 060-8638, Japan. E-mail htsutsui@med.hokudai.ac.jp

Circulation is available at http://www.circulationaha.org

DOI: 10.1161/CIRCULATIONAHA.105.582239

either a large transmural MI induced by coronary artery ligation or sham operation.

Methods

Generation of TG Mice

The rat Prx-3 cDNA fragment including the entire open reading frame from nucleotide 5 to 802 was amplified by polymerase chain reaction (PCR) and cloned into pCRII (Invitrogen, Carlsbad, Calif). An expression vector for Prx-3 was constructed with pQBI25 (TaKaRa), and the gene for green fluorescent protein was removed at the site of *Nhe*I-*Bam*HI. A cytomegalovirus promoter–driven expression cassette containing rat Prx-3 cDNA in the sense orientation was purified by ultracentrifugation with CsCl. The pronuclei of fertilized eggs from hyperovulated C57BL/6J mice were randomly microinjected with this DNA construct. Tail clips and a PCR protocol to confirm the genotype were performed by one group of investigators. Homozygous TG mice and C57BL/6J WT mice were used at 12 to 16 weeks of age. The study was approved by our institutional animal research committee and conformed to the animal care guidelines of the American Physiological Society.

Creation of MI

We created MI in 12- to 16-week-old, male TG mice (TG+MI) and nontransgenic WT littermates (WT+MI) by ligating the left coronary artery. Sham operation without coronary artery ligation was also performed in WT (WT+sham) and TG (TG+sham) mice. This assignment procedure was performed with the use of numeric codes to identify the animals.

Prx-3 Protein

Prx-3 protein levels were analyzed in cardiac tissue homogenates by Western blot analysis with a monoclonal antibody against rat Prx-3. Our preliminary studies revealed that this antibody against rat Prx-3 cross-reacted with mouse Prx-3 as a single band of 25 kDa. In brief, the LV tissues were homogenized with lysis buffer (20 mmol/L Tris-HCl, 1 mmol/L EDTA, 1 mmol/L EGTA, and 1 mmol/L phenylmethylsulfonylfluoride; pH 7.4). After centrifugation, equal amounts of protein (5 μg protein/lane), estimated by the Bradford method with a protein assay (Bio-Rad, Hercules, Calif), were electrophoresed on a 15% sodium dodecyl sulfate–polyacrylamide gel and then electrophoretically transferred to a nitrocellulose membrane (Millipore, Billerica, Mass). After being blocked with 5% nonfat milk in phosphate-buffered saline (PBS) containing 0.05% Tween 20 at 4°C for 1 hour, the membrane was incubated with the first antibody and then with the peroxidase-linked second antibody (Amersham Pharmacia, Uppsala, Sweden). Chemiluminescence was detected with an enhanced chemiluminescence Western blot detection kit (Amersham Pharmacia) according to the manufacturer's recommendation.

To further assess the subcellular localization of Prx-3 protein, mitochondrial and cytoplasmic fractions were prepared from LVs and subjected to Western blot analysis. In brief, the LV tissues were homogenized at 4°C for 1 minute in 6 volumes of buffer consisting of 10 mmol/L HEPES-NaOH (pH 7.4), 1 mmol/L disodium EDTA, and 250 mmol/L sucrose. The homogenate was centrifuged at 4°C and 3000*g* for 10 minutes to remove any nuclear and myofibrillar debris, and the resultant supernatant was centrifuged at 10 000*g* for 10 minutes to separate any cardiac subcellular fractions. The supernatant was used for the cytoplasmic fraction assay. To isolate the mitochondrial fraction, the pellet was resuspended at 4°C in a buffer consisting of 10 mmol/L HEPES-NaOH (pH 7.4), 1 mmol/L sodium EDTA, and 250 mmol/L sucrose and was washed 3 times with the same buffer. Murine antibodies directed toward glyceraldehyde 3-phosphate dehydrogenase (GAPDH) and cytochrome oxidase (COX) subunit I were also used to verify the integrity of these subcellular fractions.

Immunohistochemistry

Frozen sections of cardiac tissues were incubated in the presence of 100 nmol/L MitoTracker Red CMXRos (Molecular Probes, Eugene, Ore) at 37°C for 20 minutes. We did not repeat the freeze/thaw procedure to avoid the loss of mitochondrial integrity. After being washed with PBS (10 mmol/L sodium phosphate, pH 7.4, and 150 mmol/L NaCl), the sections were fixed with 3.7% formaldehyde for 5 minutes. After being washed, the fixed sections were incubated with 100-fold–diluted anti-rat Prx-3 antibody (10 μg/mL) in PBS at 4°C overnight. Fluorescence images were taken with a confocal laser scanning microscope (Bio-Rad MRC 1024) with laser beams of 488 and 568 nm for excitation.

Myocardial Antioxidant Enzyme Activities and Lipid Peroxidation

For the subsequent biochemical studies, the myocardial tissues with MI were carefully dissected into 3 parts: one consisting of the infarcted LV, one consisting of the border zone LV with the peri-infarct rim (a 1-mm rim of normal-appearing tissue), and one consisting of the remaining noninfarcted (remote) LV. The antioxidant enzymatic activities of superoxide dismutase (SOD), catalase, and glutathione peroxidase (GSHPx) were measured in the noninfarcted LV.[11] The formation of lipid peroxides was measured in the mitochondrial fraction isolated from the LV myocardium with use of a biochemical assay with thiobarbituric acid–reactive substances (TBARS).[4]

Survival

A survival analysis was performed in WT+sham (n=15), TG+sham (n=14), WT+MI (n=39), and TG+MI (n=37) mice. During the study period of 4 weeks, the cages were inspected daily for deceased animals. All deceased mice were examined for the presence of MI as well as pleural effusion and cardiac rupture.

Echocardiographic and Hemodynamic Measurements

At 4 weeks after surgery, echocardiographic studies were performed under light anesthesia with tribromoethanol/amylene hydrate (2.5% wt/vol, 8 μL/g IP) and spontaneous respiration. Two-dimensional, targeted M-mode tracings were recorded at a paper speed of 50 mm/s. Under the same anesthesia with Avertin, a 1.4F micromanometer-tipped catheter (Millar Instruments, Houston, Tex) was inserted into the right carotid artery and then advanced into the LV to measure LV pressures. One subset of investigators who were not informed of the experimental group assignments performed the in vivo LV function studies.

Infarct Size

To measure infarct size 28 days after MI, the heart was excised and the LVs were cut from apex to base into 3 transverse sections. Five-micron sections were cut and stained with Masson's trichrome. Infarct length was measured along the endocardial and epicardial surfaces in each of the cardiac sections, and the values from all specimens were summed. Infarct size (as a percentage) was calculated as total infarct circumference divided by total cardiac circumference.[12]

In addition, to measure infarct size after 24 hours (when most animals were still alive), a separate group of animals including WT+MI (n=5) and TG+MI (n=5) mice was created by ligating the left coronary artery according to the same methods described earlier. After 24 hours of coronary artery ligation, Evans blue dye (1%) was perfused into the aorta and coronary arteries, and tissue sections were weighed and then incubated with a 1.5% triphenyltetrazolium chloride solution. The infarct area (pale), the area at risk (not blue), and the total LV area from each section were measured.[13] In our preliminary study, we confirmed excellent reliability of infarct size measurements, in which a morphometric method similar to that performed in this study was used. The intraobserver and interob-

server variabilities between 2 measurements divided by these means, expressed as a percentage, were each <5%.

Myocardial Histopathology and Apoptosis

Myocyte cross-sectional area and collagen volume fraction were determined by quantitative morphometry of tissue sections from the mid-LV. To detect apoptosis, tissue sections from the mid-LV were stained with terminal deoxynucleotidyl transferase–mediated dUTP nick end-labeling (TUNEL) staining. The number of TUNEL-positive cardiac myocyte nuclei was counted, and the data were normalized per 10^5 total nuclei identified by hematoxylin-positive staining in the same sections. The proportion of apoptotic cells was counted in the noninfarcted LV. We further examined whether apoptosis was present by the more sensitive ligation-mediated PCR fragmentation assays (Maxim Biotech, Inc, Rockville, Md).

mtDNA Copy Number

DNA was extracted from cardiac tissues, and a Southern blot analysis was performed to measure the mtDNA copy number, as described earlier.[4] Primers for the mtDNA probe corresponded to nucleotides 2424 to 3605 of the mouse mitochondrial genome, and those for the nuclear-encoded mouse 18S rRNA probe corresponded to nucleotides 435 to 1951 of the human 18S rRNA genome. The mtDNA levels were normalized to the abundance of the 18S rRNA gene run on the same gel.

Mitochondrial Complex Enzyme Activity

The specific activity of mitochondrial electron transport chain complex I (rotenone-sensitive NADH-ubiquinone oxidoreductase), complex II (succinate-ubiquinone oxidoreductase), complex III (ubiquinol–cytochrome *c* oxidoreductase), and complex IV (cytochrome *c* oxidase) was measured in myocardial tissues according to methods described previously.[4] All enzymatic activities were expressed as nanomoles per minute per milligram protein.

Plasma TBARS

The formation of TBARS in peripheral blood samples from WT+MI and TG+MI mice was measured by a fluorometric assay, as described previously.[14] In brief, 100 μL of whole blood was mixed with 1 mL of saline and centrifuged at 3000*g* for 15 minutes. The supernatant was mixed with $1/12$N H_2SO_4 and 10% phosphotungstic acid, and the mixture was centrifuged. The sediment was suspended in distilled water, 0.3% thiobarbituric acid, and 0.1% butylated hydroxytoluene. The reaction mixture was then heated at 100°C for 60 minutes in an oil bath. After being cooled with tap water, the mixture was extracted with *n*-butanol and centrifuged at 1600*g* for 15 minutes. The fluorescence intensity of the organic phase was measured by spectrofluorometry with a wavelength of 510-nm excitation and 550-nm emission. Malondialdehyde standards (Sigma-Aldrich, St. Louis, Mo) were included with each assay batch, and plasma TBARS were expressed as micromoles per gram of plasma protein in reference to these standards.

Statistical Analysis

Data are expressed as mean±SEM. Survival analysis was performed by the Kaplan-Meier method, and between-group differences in survival were tested by the log-rank test. A between-group comparison of means was performed by 1-way ANOVA, followed by *t* tests. The Bonferroni correction was applied for multiple comparisons of means. $P<0.05$ was considered statistically significant.

The authors had full access to the data and take full responsibility for their integrity. All authors have read and agreed to the manuscript as written.

Results

We investigated 4 groups of mice, WT+sham (n=15), TG+sham (n=14), WT+MI (n=39), and TG+MI (n=37), in the present study. A survival analysis was performed for all of these mice. Subsequent echocardiographic and hemodynamic measurements were performed in the 4-week survivors: 15 WT+sham, 14 TG+sham, 25 WT+MI, and 31 TG+MI mice. These measurements could not be accomplished in 4 WT+MI and 5 TG+MI mice owing to technical difficulties. Survivor mice were further divided into 2 groups: those studied for subsequent histological analysis, including infarct size, myocyte size, and collagen volume fraction measurements as well as TUNEL staining (5 WT+sham, 5 TG+sham, 8 WT+MI, and 8 TG+MI), and those for the biochemical assay, including antioxidant enzyme activity, Prx-3 protein levels, mitochondrial lipid peroxidation, mtDNA copy number, and mitochondrial complex enzyme activities (8 WT+sham, 8 TG+sham, 8 WT+MI, and 8 TG+MI). Infarct size was not measured in the mice that died.

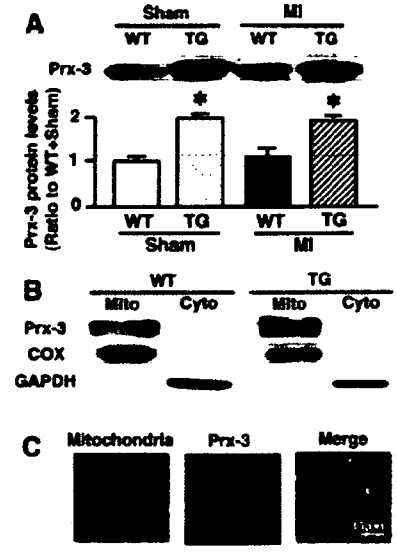

Figure 1. A, Representative Western blot analysis of Prx-3 protein levels (upper panels) and summary data (lower panels) in hearts from WT+sham, TG+sham, WT+MI, and TG+MI mice (n=6 each). Total protein extracts from the hearts were probed with a monoclonal antibody against rat Prx-3. The antibody recognized both rat and mouse Prx-3 as a single band of 25k Da. Data were obtained by densitometric quantification of the Western blots. Values are expressed as the ratio to the WT+sham value and mean±SEM. *$P<0.05$ for the difference from the ratio to WT+sham values. B, Localization of Prx-3 to mitochondria (mito). Western blot analysis of mitochondrial and cytoplasmic (cyto) fractions that were probed with antibodies directed toward Prx-3 as well as specific mitochondrial and cytoplasmic markers: GAPDH was detected in the cytoplasmic but not the mitochondrial fraction, and COX subunit I was detected in the mitochondrial but not the cytoplasmic fraction. Importantly, Prx-3 proteins were detected only in the mitochondrial fraction but not in the cytoplasmic fraction. C, Myocardial tissue sections from TG mice were doubly stained with MitoTracker dye (red) and a rat Prx-3–specific antibody (green). Immunoreactivity for Prx-3 was observed in the cytoplasm of cardiac myocytes. The merged images show that Prx-3 colocalized with the mitochondria (yellow). Scale bar=10 μm.

Myocardial Antioxidants and TBARS

First, baseline differences in Prx-3 proteins as well as other antioxidant enzyme activities between WT and TG mice were determined. In TG+sham, there was a significant increase in Prx-3 protein levels in the LV compared with that of WT+sham (Figure 1A). Importantly, the antioxidants, in-

TABLE 1. Characteristics of Animal Models

	WT+Sham	TG+Sham	WT+MI	TG+MI
Antioxidant enzymes				
n	7	7	7	7
SOD, U/mg protein	26.4±1.1	27.8±1.4	25.1±1.7	23.9±1.2
GSHPx, nmol/min per mg protein	74.1±3.2	77.7±6.7	87.8±4.8	86.1±4.2
Catalase, nmol/mg protein	79.9±6.4	85.0±6.2	87.1±3.5	81.4±5.8
Echocardiographic data				
n	15	14	21	26
Heart rate, bpm	481±11	451±8	463±13	458±8
LVEDD, mm	3.47±0.05	3.37±0.08	5.51±0.13†	4.9±0.10†§
LVESD, mm	2.22±0.05	2.12±0.10	4.78±0.13†	4.08±0.10†§
Fractional shortening, %	35.3±0.8	37.0±1.1	13.1±0.6†	16.9±0.6†§
Hemodynamic data				
n	15	14	21	26
Heart rate, bpm	447±14	455±14	453±9	466±7
Mean aortic pressure, mm Hg	83±3	78±2	76±2	77±3
LVEDP, mm Hg	2.7±0.5	2.5±0.3	11.4±1.5†	7.6±1.0*‡
Organ weight data				
n	15	14	21	26
Body wt, g	26.9±0.5	27.0±0.8	27.0±0.3	26.4±0.4
LV wt/body wt, mg/g	3.2±0.1	3.0±0.1	4.6±0.3†	4.4±0.1†
Lung wt/body wt, mg/g	5.0±0.1	5.2±0.1	7.6±0.5†	6.4±0.3†‡
Pleural effusion, %	0	0	43	15‡

EDD indicates end-diastolic diameter; ESD, end-systolic diameter; and wt, weight. Values are mean±SEM.

*P<0.05, †P<0.01 vs WT+Sham. ‡P<0.05, §P<0.01 vs WT+MI.

cluding SOD, GSHPx, and catalase activities, were not altered in the TG hearts (Table 1), indicating no effects of Prx-3 overexpression on other antioxidant enzymes. Second, the changes in antioxidants after MI were assessed. Prx-3 protein levels were significantly higher in TG+MI than in WT+MI (Figure 1A) mice. The activities of other antioxidant enzymes were not altered in WT+MI or TG+MI compared with WT+sham animals (Table 1).

The cytoplasmic marker GAPDH was detected exclusively in the cytoplasmic but not in the mitochondrial fraction, whereas COX subunit I was detected preferentially in the mitochondrial but not in the cytoplasmic fraction. This substantiates the integrity of our cellular fractions. Importantly, Prx-3 was detected only in the mitochondrial fraction but not in the cytoplasmic fraction, further confirming that Prx-3 was localized exclusively in the mitochondria (Figure 1B). In addition, immunohistochemical studies showed a homogeneous Prx-3 distribution in cardiac myocytes that colocalized with the mouse mitochondria (Figure 1C). Prx-3 staining showed a relatively spotty pattern. These results further confirm that the rat Prx-3 transgene is not expressed in the cytoplasm within the mouse heart. Mitochondrial TBARS measured in the noninfarcted LV were significantly greater in WT+MI compared with sham animals and were significantly lower in the TG+MI group (Figure 2).

Survival

There were no deaths in the sham-operated groups. Early operative mortality (within 6 hours) was comparable between WT+MI and TG+MI animals (15% versus 7%; P=NS). The survival rate up to 4 weeks tended to be higher in TG+MI compared with WT+MI mice, but this difference did not reach statistical significance (P=0.06 by log-rank test; Figure 3A). Death was suspected to be attributable to heart failure and/or arrhythmia. Five WT+MI (15%) and 2 TG+MI (5%) mice died of LV rupture (P=NS).

Infarct Size

Infarct size as determined by morphometric analysis 28 days after MI was comparable (55±1% versus 56±1%; P=0.83) between WT+MI (n=6) and TG+MI (n=6) groups. To further confirm that overexpression of Prx-3 did not alter infarct size, both the area at risk and infarct area were

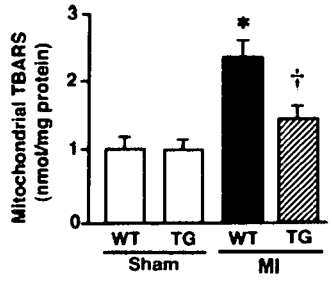

Figure 2. Mitochondrial TBARS in 4 experimental groups of animals (n=8 each). Values are mean±SEM. *P<0.05 for difference from the WT+sham value. †P<0.05 for difference from the WT+MI value.

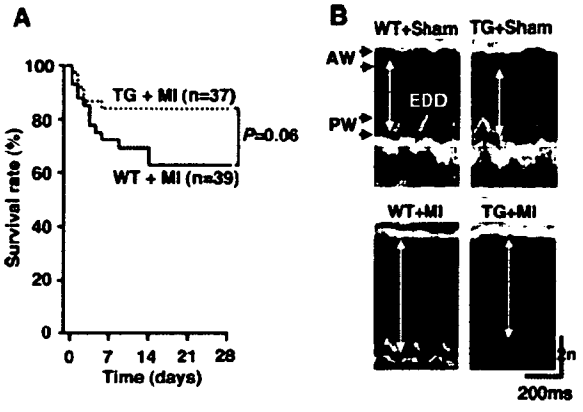

Figure 3. A, Kaplan-Meier survival analysis. Percentages of surviving WT+MI (n=39) and TG+MI (n=37) mice were plotted. Between-group difference was tested by the log-rank test. B, M-mode echocardiograms obtained from WT+sham, TG+sham, WT+MI, and TG+MI mice. AW indicates anterior wall; PW, posterior wall; and EDD, end-diastolic diameter.

measured in mice 24 hours after coronary artery ligation. Percentages of the LV at risk (risk area/LV, 51±3% versus 52±2%; P=0.89) and infarct size (infarct/risk area, 79±1% versus 78±1%; P=0.13) were also comparable between WT+MI (n=5) and TG+MI (n=5) animals.

Echocardiography and Hemodynamics

The echocardiographic and hemodynamic data of surviving mice at 28 days are shown in Figure 3B and Table 1. LV diameters were significantly larger in WT+MI mice with respect to WT+sham animals. TG+MI mice displayed less LV cavity dilatation and greater fractional shortening than did WT+MI mice. There was no significant difference in heart rate or aortic blood pressure among the 4 groups of mice. LV end-diastolic pressure (LVEDP) was higher in WT+MI than in WT+sham animals, but this increase was significantly attenuated in TG+MI mice.

Organ Weights and Histomorphometry

Coincident with an increased LVEDP, lung weight/body weight was larger in WT+MI mice, and this increase was attenuated in TG+MI mice (Table 1). The prevalence of pleural effusion was also lower in TG+MI than in WT+MI groups. Histomorphometric analysis of noninfarcted LV sections showed that myocyte cross-sectional area was greater in WT+MI mice but was significantly attenuated in TG+MI mice (Figure 4). Collagen volume fraction was greater in WT+MI mice, but this change was inhibited in TG+MI mice (Figure 4).

Myocardial Apoptosis

There were rare TUNEL-positive nuclei in sham-operated mice. The number of TUNEL-positive myocytes in the noninfarcted LV was larger in WT+MI mice but was significantly smaller in TG+MI animals (Figure 5A). In addition, the intensity of the DNA ladder indicated that apoptosis in TG+MI animals was decreased compared with that in WT+MI mice (Figure 5B).

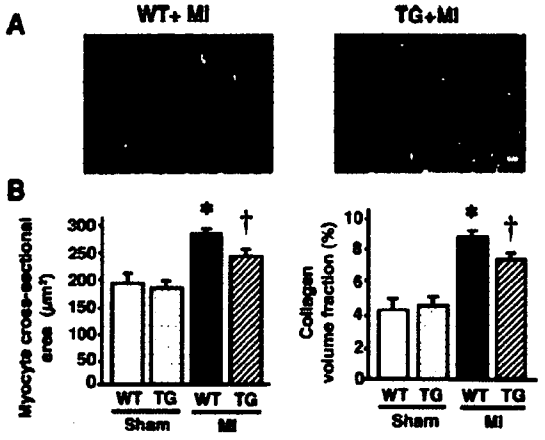

Figure 4. A, Photomicrographs of Masson trichrome–stained LV cross sections obtained from WT+MI and TG+MI mice. Scale bar=10 μm. B, Myocyte cross-sectional area and collagen volume fraction in WT+sham (n=5), TG+sham (n=5), WT+MI (n=8), and TG+MI (n=8) mice. Values are mean±SEM. *P<0.05 for difference from the WT+sham value. †P<0.05 for difference from the WT+MI value.

mtDNA and Mitochondrial Complex Enzymes Activity

Consistent with our previous studies,[4] mtDNA copy number in the noninfarcted LV from WT+MI animals showed a 36% decrease (P<0.05) compared with that in sham-operated mice, which was significantly prevented and was preserved at normal levels in TG+MI animals (Figure 6).

To determine the effects of mtDNA alterations on mitochondrial function, we next measured the mitochondrial electron transport chain complex enzyme activities. The enzymatic activities of complexes I, III, and IV were significantly lower in the noninfarcted LV from WT+MI than in those from WT+sham animals (Table 2). Most important, no such decrease was observed in TG+MI mice. The enzymatic activity of complex II, exclusively encoded by nuclear DNA, was not altered in either group. These results indicate that mtDNA copy number and mitochondrial complex enzymatic activities are downregulated in the post-MI heart and that Prx-3 gene overexpression efficiently counteracts these mitochondrial deficiencies.

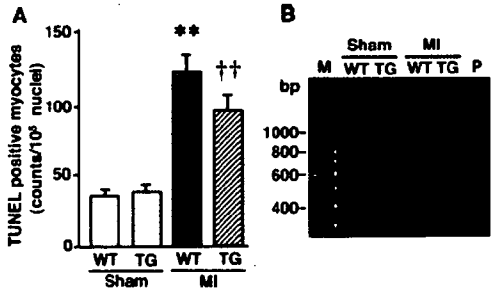

Figure 5. A, Numbers of TUNEL-positive myocytes in the noninfarcted LV from WT+sham, TG+sham, WT+MI, and TG+MI mice (n=5 each). Values are mean±SEM. **P<0.01 for the difference from the WT+sham value. ††P<0.01 for the difference from the WT+MI value. B, DNA ladder indicative of apoptosis in the genomic DNA from the LV. M indicates marker; P, positive control.

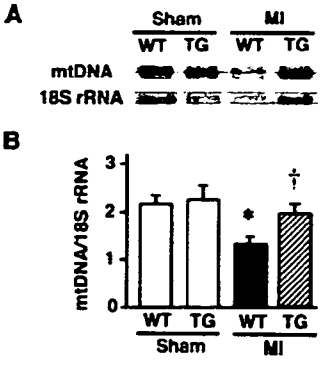

Figure 6. A, Southern blot analysis of mtDNA copy number in total DNA extracts from the hearts from WT+sham, TG+sham, WT+MI, and TG+MI mice. Top bands show signals from the mtDNA fragments, and bottom bands show signals from the nuclear DNA fragments containing the 18S rRNA gene. B, Summary data for a Southern blot analysis of mtDNA copy number in 4 groups of animals (n=8 each). Data were obtained by densitometric quantification of the Southern blots, such as shown in A. Values are expressed as the ratio to WT+sham values and mean±SEM. *$P<0.05$ for the difference from the WT+sham value. †$P<0.05$ for the difference from the WT+MI value.

Plasma TBARS

Plasma TBARS were comparable between WT+MI and TG+MI mice (0.46±0.04 versus 0.54±0.05 μmol/g protein; P=NS).

Discussion

The present study provides the first direct evidence that overexpression of mitochondrial antioxidant Prx-3 protects the heart against post-MI remodeling and failure in mice. It reduced LV cavity dilatation and dysfunction, as well as myocyte hypertrophy, interstitial fibrosis, and apoptosis of the noninfarcted myocardium. These beneficial effects of *Prx-3* gene overexpression were associated with an attenuation of mitochondrial oxidative stress, mtDNA decline, and dysfunction. They were not due to its MI size-sparing effect but occurred secondary to more adaptive remodeling.

Mitochondria are the predominant source of ROS in the failing myocardium.[1] Most of the $\cdot O_2^-$ generated by the mitochondria is vectorially released into the mitochondrial matrix. $\cdot O_2^-$ impairs mitochondrial function by oxidizing the Fe-S centers of complex enzymes. In addition, $\cdot O_2^-$ is converted to peroxynitrite, an extremely powerful oxidant, as a result of its reaction with NO produced by mitochondrial NO synthase. $\cdot O_2^-$ is also converted to H_2O_2 by a specific intramitochondrial Mn-SOD. Although Mn-SOD relieves mitochondrial oxidative stress caused by $\cdot O_2^-$, it generates H_2O_2 and therefore, further enhances a different type of oxidative stress. H_2O_2 can damage cellular macromolecules such as proteins, lipids, and nucleic acids, especially after its conversion to ·OH. Moreover, these increased ROS in the mitochondria were associated with a decreased mtDNA copy number and reduced oxidative capacity owing to low complex enzyme activities.[4] Therefore, chronic increases in mitochondrial ROS production cause mtDNA damage and dysfunction, which thus, can lead to a catastrophic cycle of further oxidative stress and ultimate cellular injury.[5] This deleterious process may play an important role in the development and progression of myocardial remodeling and failure.[4] Based on these results, mitochondrial antioxidants are expected to be the first line-of-defense mechanism against ROS generation in the mitochondria and ROS-mediated mitochondrial injury and thus, may protect the heart from adverse remodeling and failure.

Prx-3, which was formerly known as SP-22, or MER5, is currently identified as a mitochondrial member of the novel antioxidant proteins designated as Prxs.[15] Among 6 known mammalian Prxs, Prx-1 to -4 require the small redox protein thioredoxin (Trx) as an electron donor to remove H_2O_2, whereas Prx-5 and -6 can use other cellular reductants, such as GSH, as their electron donor.[16] Prx-1, -2, and -6 are found in the cytoplasm and nucleus,[7] whereas Prx-3 contains a mitochondrial localization sequence, is found exclusively in the mitochondria, and uses mitochondrial Trx-2 as the electron donor for its peroxidase activity.[17] It functions not only by removing H_2O_2 formed after the SOD-catalyzed dismutation reaction but also by detoxifying peroxynitrite.[6] Therefore, the great efficiency of Prx-3 as an antioxidant shown in the present study may be attributable to the fact that it is located in the mitochondria and can utilize lipid peroxides as well as H_2O_2 for substrates. In fact, overexpression of Prx-3 has been shown to protect thymoma cells from apoptosis induced by hypoxia, a bolus of peroxide, or an anticancer drug.[18] Moreover, Prx-3 overexpression has been reported to protect rat hippocampal neurons from excitotoxic injury.[8] Prx-5 is also associated with the mitochondria in addition to the peroxisomes and nucleus. Recently, increased expression of Prx-5 was found to have protected Chinese hamster ovary cells from mtDNA damage induced by oxidative stress.[19] Therefore, Prx-5 may also exert beneficial effects against mitochondrial oxidative stress in post-MI hearts.

GSHPx also catalyzes the reduction of H_2O_2. In fact, our previous studies demonstrated that overexpression of GSHPx

TABLE 2. Mitochondrial Complex Enzyme Activities

	WT+Sham	TG+Sham	WT+MI	TG+MI
n	7	7	7	7
Complex I, nmol/min per mg protein	282±26	265±38	159±25*	287±16†
Complex II, nmol/min per mg protein	770±70	718±93	711±85	726±128
Complex III, nmol/min per mg protein	505±11	470±31	367±20*	451±21†
Complex IV, nmol/min per mg protein	1223±37	1175±34	744±68*	939±54†

Values are mean±SEM.
*$P<0.05$ vs WT+sham; †$P<0.05$ vs WT+MI.

inhibited LV remodeling and failure after MI.[13] However, GSHPx is located predominantly in the cytosol, and only a small proportion (≈10%) is present in the mitochondria.[20] Therefore, it remains unclear whether the beneficial effects of GSHPx overexpression on post-MI hearts were attributable to an increase of this enzyme in the cytosol, the mitochondria, or both. The specific localization of Prx-3 in the mitochondria suggests that mitochondrial oxidative stress plays an important role in the development and progression of heart failure, and antioxidants localized specifically within the mitochondria provide a primary line of defense against this disease process.

A growing body of evidence suggests that ROS play a major role in the pathogenesis of cardiac failure. Furthermore, antioxidants have been shown to exert protective and beneficial effects against heart failure.[21,22] A previous study from our laboratory demonstrated that dimethylthiourea improved survival and prevented LV remodeling and failure after MI.[10] However, the most effective way to evaluate the contribution of any specific antioxidant and obtain direct evidence of an adverse role for ROS in heart failure is through gene manipulation. Therefore, the present study not only extends the previous observation that used antioxidants but also reveals the major role of mitochondrial oxidative stress in the pathophysiology of post-MI remodeling and failure.

The beneficial effects of Prx-3 overexpression shown in the present study were not due to its MI size-sparing effect, because there was no statistically significant difference in infarct size between WT+MI and TG+MI mice. Furthermore, its effects were not attributable to hemodynamics because blood pressures and heart rates were not altered (Table 1). Importantly, it is also unlikely that these effects were caused by the altered expression of antioxidant enzymes other than Prx-3 (Table 1). Moreover, the beneficial effects of Prx-3 overexpression were not due to systemic induction of antioxidant defenses. This possibility is less likely because plasma TBARS were comparable between WT+MI and TG+MI mice. Nevertheless, we cannot completely exclude the possibility that the systemic effects of Prx-3 induction might also have contributed to this phenotype because this TG is not heart-specific.

There may be several factors contributing to the protective effects conferred by Prx-3 overexpression on post-MI remodeling and failure. First, recent studies have demonstrated that a Trx-related antioxidant system is closely associated with the regulation of apoptosis, probably through quenching of ROS and redox control of the mitochondrial permeability transition pores that release cytochrome *c*.[23] A subtle increase in ROS caused by partial inhibition of SOD results in apoptosis in isolated cardiac myocytes.[24] Previous studies have demonstrated that apoptosis appears not only in infarcted but also in noninfarcted myocardium after MI.[25] Specifically, apoptosis occurs in the noninfarcted LV late after MI. This is an intriguing observation, in light of the remodeling process known to occur within the noninfarcted area, which is characterized by the loss of myocytes and hypertrophy. In fact, recent studies have suggested cardiac myocyte apoptosis contributes to LV remodeling after MI.[26,27] Importantly, increased oxidative stress occurs concomitantly with increased cardiac myocyte apoptosis within the noninfarcted area. This is a provoking observation, because oxidative stress is a powerful inducer of apoptotic cell death.[28] The present study suggests that the coexistence of oxidative stress and myocyte apoptosis in the noninfarcted LV after MI is causally related. Oxidative stress may mediate myocyte apoptosis, which may lead to myocardial remodeling and failure. Therefore, the decreased mitochondrial oxidative stress due to Prx-3 overexpression could contribute to the amelioration of apoptosis (Figure 5) and eventual post-MI cardiac failure. Second, Prx-3 overexpression prevented the decrease in mtDNA copy number (Figure 6) as well as mitochondrial complex enzyme activities (Table 2). Our previous studies have demonstrated an intimate link between mtDNA damage, increased lipid peroxidation, and a decrease in mitochondrial function, which might play a major role in the development and progression of cardiac failure.[4]

There are several issues to be acknowledged as limitations of this study. First, the differences between WT+MI and TG+MI groups in their echocardiographic measurements are not remarkable, even though they are statistically significant (Table 1). However, our previous study showed that the intraobserver and interobserver variabilities in our echocardiographic measurements for LV dimensions were small, and measurements made in the same animals on separate days were highly reproducible.[12] Therefore, these values are considered to be valid. Second, longer-term follow-up data are not available for the animals in the current study. We therefore could not determine whether the differences between WT+MI and TG+MI groups seen in the present study were more or less significant at later time points, when additional LV remodeling would have been expected to occur.

In conclusion, Prx-3 overexpression inhibited the development of LV remodeling and failure after MI, which was associated with an attenuation of myocyte hypertrophy, apoptosis, and interstitial fibrosis. It also ameliorated mitochondrial oxidative stress as well as mtDNA decline and mitochondrial dysfunction in post-MI hearts. Therapies designed to interfere with mitochondrial oxidative stress could be beneficial to prevent heart failure after MI.

Acknowledgments

This study was supported in part by grants from the Ministry of Education, Science and Culture (No. 12670676, 14370230, 17390223). A portion of this study was conducted at Kyushu University Station for Collaborative Research I and II.

Disclosures

None.

References

1. Ide T, Tsutsui H, Kinugawa S, Suematsu N, Hayashidani S, Ichikawa K, Utsumi H, Machida Y, Egashira K, Takeshita A. Direct evidence for increased hydroxyl radicals originating from superoxide in the failing myocardium. *Circ Res.* 2000;86:152–157.
2. Mallat Z, Philip I, Lebret M, Chatel D, Maclouf J, Tedgui A. Elevated levels of 8-iso-prostaglandin F2α in pericardial fluid of patients with heart failure: a potential role for in vivo oxidant stress in ventricular dilatation and progression to heart failure. *Circulation.* 1998;97:1536–1539.

3. Ide T, Tsutsui H, Kinugawa S, Utsumi H, Kang D, Hattori N, Uchida K, Arimura K, Egashira K, Takeshita A. Mitochondrial electron transport complex I is a potential source of oxygen free radicals in the failing myocardium. *Circ Res.* 1999;85:357–363.
4. Ide T, Tsutsui H, Hayashidani S, Kang D, Suematsu N, Nakamura K, Utsumi H, Hamasaki N, Takeshita A. Mitochondrial DNA damage and dysfunction associated with oxidative stress in failing hearts after myocardial infarction. *Circ Res.* 2001;88:529–535.
5. Suematsu N, Tsutsui H, Wen J, Kang D, Ikeuchi M, Ide T, Hayashidani S, Shiomi T, Kubota T, Hamasaki N, Takeshita A. Oxidative stress mediates tumor necrosis factor-α–induced mitochondrial DNA damage and dysfunction in cardiac myocytes. *Circulation.* 2003;107:1418–1423.
6. Bryk R, Griffin P, Nathan C. Peroxynitrite reductase activity of bacterial peroxiredoxins. *Nature.* 2000;407:211–215.
7. Kang SW, Chae HZ, Seo MS, Kim K, Baines IC, Rhee SG. Mammalian peroxiredoxin isoforms can reduce hydrogen peroxide generated in response to growth factors and tumor necrosis factor-α. *J Biol Chem.* 1998;273:6297–6302.
8. Hattori F, Murayama N, Noshita T, Oikawa S. Mitochondrial peroxiredoxin-3 protects hippocampal neurons from excitotoxic injury in vivo. *J Neurochem.* 2003;86:860–868.
9. Sia YT, Lapointe N, Parker TG, Tsoporis JN, Deschepper CF, Calderone A, Pourdjabbar A, Jasmin JF, Sarrazin JF, Liu P, Adam A, Butany J, Rouleau JL. Beneficial effects of long-term use of the antioxidant probucol in heart failure in the rat. *Circulation.* 2002;105:2549–2555.
10. Kinugawa S, Tsutsui H, Hayashidani S, Ide T, Suematsu N, Satoh S, Utsumi H, Takeshita A. Treatment with dimethylthiourea prevents left ventricular remodeling and failure after experimental myocardial infarction in mice: role of oxidative stress. *Circ Res.* 2000;87:392–398.
11. Ho YS, Magnenat JL, Bronson RT, Cao J, Gargano M, Sugawara M, Funk CD. Mice deficient in cellular glutathione peroxidase develop normally and show no increased sensitivity to hyperoxia. *J Biol Chem.* 1997;272:16644–16651.
12. Shiomi T, Tsutsui H, Hayashidani S, Suematsu N, Ikeuchi M, Wen J, Ishibashi M, Kubota T, Egashira K, Takeshita A. Pioglitazone, a peroxisome proliferator–activated receptor-γ agonist, attenuates left ventricular remodeling and failure after experimental myocardial infarction. *Circulation.* 2002;106:3126–3132.
13. Shiomi T, Tsutsui H, Matsusaka H, Murakami K, Hayashidani S, Ikeuchi M, Wen J, Kubota T, Utsumi H, Takeshita A. Overexpression of glutathione peroxidase prevents left ventricular remodeling and failure after myocardial infarction in mice. *Circulation.* 2004;109:544–549.
14. Ide T, Tsutsui H, Ohashi N, Hayashidani S, Suematsu N, Tsuchihashi M, Tamai H, Takeshita A. Greater oxidative stress in healthy young men compared with premenopausal women. *Arterioscler Thromb Vasc Biol.* 2002;22:438–442.
15. Wood ZA, Schroder E, Robin Harris J, Poole LB. Structure, mechanism and regulation of peroxiredoxins. *Trends Biochem Sci.* 2003;28:32–40.
16. Fisher AB, Dodia C, Manevich Y, Chen JW, Feinstein SI. Phospholipid hydroperoxides are substrates for non-selenium glutathione peroxidase. *J Biol Chem.* 1999;274:21326–21334.
17. Watabe S, Hiroi T, Yamamoto Y, Fujioka Y, Hasegawa H, Yago N, Takahashi SY. SP-22 is a thioredoxin-dependent peroxide reductase in mitochondria. *Eur J Biochem.* 1997;249:52–60.
18. Nonn L, Berggren M, Powis G. Increased expression of mitochondrial peroxiredoxin-3 (thioredoxin peroxidase-2) protects cancer cells against hypoxia and drug-induced hydrogen peroxide–dependent apoptosis. *Mol Cancer Res.* 2003;1:682–689.
19. Banmeyer I, Marchand C, Clippe A, Knoops B. Human mitochondrial peroxiredoxin 5 protects from mitochondrial DNA damages induced by hydrogen peroxide. *FEBS Lett.* 2005;579:2327–2333.
20. Chang TS, Cho CS, Park S, Yu S, Kang SW, Rhee SG. Peroxiredoxin III, a mitochondrion-specific peroxidase, regulates apoptotic signaling by mitochondria. *J Biol Chem.* 2004;279:41975–41984.
21. Dhalla AK, Hill MF, Singal PK. Role of oxidative stress in transition of hypertrophy to heart failure. *J Am Coll Cardiol.* 1996;28:506–514.
22. Nakamura R, Egashira K, Machida Y, Hayashidani S, Takeya M, Utsumi H, Tsutsui H, Takeshita A. Probucol attenuates left ventricular dysfunction and remodeling in tachycardia-induced heart failure: roles of oxidative stress and inflammation. *Circulation.* 2002;106:362–367.
23. Petronilli V, Costantini P, Scorrano L, Colonna R, Passamonti S, Bernardi P. The voltage sensor of the mitochondrial permeability transition pore is tuned by the oxidation-reduction state of vicinal thiols: increase of the gating potential by oxidants and its reversal by reducing agents. *J Biol Chem.* 1994;269:16638–16642.
24. Siwik DA, Tzortzis JD, Pimental DR, Chang DL, Pagano PJ, Singh K, Sawyer DB, Colucci WS. Inhibition of copper-zinc superoxide dismutase induces cell growth, hypertrophic phenotype, and apoptosis in neonatal rat cardiac myocytes in vitro. *Circ Res.* 1999;85:147–153.
25. Palojoki E, Saraste A, Eriksson A, Pulkki K, Kallajoki M, Voipio-Pulkki LM, Tikkanen I. Cardiomyocyte apoptosis and ventricular remodeling after myocardial infarction in rats. *Am J Physiol Heart Circ Physiol.* 2001;280:H2726–H2731.
26. Sam F, Sawyer DB, Chang DL, Eberli FR, Ngoy S, Jain M, Amin J, Apstein CS, Colucci WS. Progressive left ventricular remodeling and apoptosis late after myocardial infarction in mouse heart. *Am J Physiol Heart Circ Physiol.* 2000;279:H422–H428.
27. Oskarsson HJ, Coppey L, Weiss RM, Li WG. Antioxidants attenuate myocyte apoptosis in the remote non-infarcted myocardium following large myocardial infarction. *Cardiovasc Res.* 2000;45:679–687.
28. von Harsdorf R, Li PF, Dietz R. Signaling pathways in reactive oxygen species–induced cardiomyocyte apoptosis. *Circulation.* 1999;99:2934–2941.

CLINICAL PERSPECTIVE

A growing body of evidence suggests that oxidative stress, an excess generation of reactive oxygen species (ROS), plays a major role in the pathogenesis of heart failure. Furthermore, antioxidants have been shown to exert protective and beneficial effects against this process. Recent studies have suggested that mitochondria are the predominant source of ROS in the failing heart, and mitochondrial antioxidants are expected to be the first line of defense against mitochondrial oxidative stress–mediated myocardial injury. The present study demonstrated that overexpression of peroxiredoxin-3 (Prx-3) inhibited cardiac remodeling and failure after myocardial infarction (MI) created by ligation of the left coronary artery in mice. Prx-3 contains a mitochondrial localization sequence, is found exclusively in the mitochondria, and uses mitochondrial thioredoxin (Trx)-2 as the electron donor for its peroxidase activity. It functions not only by removing H_2O_2 formed after the superoxide dismutase (SOD)–catalyzed dismutation reaction but also by detoxifying peroxynitrite. Therefore, the great efficiency of Prx-3 as an antioxidant shown in the present study may be attributable to the fact that it is located in the mitochondria and can utilize lipid peroxides as well as H_2O_2 for substrates. The present study not only extends previous investigations that used antioxidants but also reveals a major role for mitochondrial oxidative stress in the pathophysiology of postinfarct heart failure. Therapies designed to interfere with mitochondrial oxidative stress by using antioxidant Prx-3 might also beneficial in preventing clinical heart failure.

β2-Adrenergic Agonists Suppress Rat Autoimmune Myocarditis

Potential Role of β2-Adrenergic Stimulants as New Therapeutic Agents for Myocarditis

Mototsugu Nishii, PhD, MD; Takayuki Inomata, MD, PhD; Hiroe Niwano, MD, PhD; Hitoshi Takehana, MD, PhD; Ichiro Takeuchi, MD, PhD; Hironari Nakano, MD, PhD; Hisahito Shinagawa, MD; Takashi Naruke, MD; Toshimi Koitabashi, MD, PhD; Jun-ichi Nakahata, MD; Tohru Izumi, MD, PhD

Background—The therapeutic potential of β2-adrenergic receptor (AR) agonists in the treatment of autoimmune diseases has been reported. However, the role of these drugs in the myocardial structure–induced autoimmune process, which is thought to play a crucial role in the progression of myocarditis to subsequent complications, has not been elucidated.

Methods and Results—Experimental autoimmune myocarditis (EAM) was induced in rats by immunization with cardiac myosin. On daily administration from day 0 after immunization, the β2-selective AR agonists formoterol or salbutamol ameliorated EAM on day 21 and increased myocardial interleukin-10/interferon-γ mRNA levels. Propranolol, a nonselective β-AR antagonist, aggravated EAM on day 21 and decreased mRNA levels, whereas metoprolol, a β1-selective AR antagonist, showed no effect. These results were reflected in vivo by the proliferation of cardiac myosin–primed lymph node cells from drug-treated rats. In vitro addition of β2-selective AR agonists inhibited the activation of cardiac myosin fragment–specific myocarditogenic T lymphocytes, and this effect was reversed by ICI118,551, a β2-selective AR antagonist. Furthermore, treatment with 2 different β2-selective AR agonists starting on day 14 also ameliorated EAM on day 21.

Conclusions—β2-AR stimulation suppressed the development of EAM by inhibiting cardiac myosin–specific T-lymphocyte activation in lymphoid organs and by shifting the imbalance in Th1/Th2 cytokine toward Th2 cytokine. Furthermore, it also ameliorated established myocardial inflammation. β2-AR–stimulating agents may represent important immunomodulators of the cardiac myosin–induced autoimmune process and have potential as a new therapy for myocarditis. (***Circulation.* 2006;114:936-944.**)

Key Words: immune system ■ myocarditis ■ receptors, adrenergic, beta

Apart from those with fulminant cases requiring mechanical circulatory support for severely deteriorated circulatory collapse, most patients with acute myocarditis recover rapidly to an uncomplicated status, with cessation of myocardial inflammation and a generally favorable outcome.[1] Some patients, however, progress to persistent myocardial inflammation and subsequent dilated cardiomyopathy.[2,3] Although chronic viral infection has long been recognized as a candidate causative factor for these pathophysiological mechanisms,[3] a number of experimental models have demonstrated the crucial role[4,5] of myocardial structure–mediated autoimmune processes, which follow the myocardial damage provoked by the initial viral infection.[6,7] The presence of autoantibodies against myocardial structure in patients with myocarditis and dilated cardiomyopathy[8,9] supports the involvement of myocardial structure–mediated autoimmune processes in these settings in humans.

Clinical Perspective p 944

Investigations using rat experimental autoimmune myocarditis (EAM) have shown that Th1 cytokines such as interferon-γ (IFN-γ) and interleukin-12 (IL-12) are major promoters of these autoimmune processes.[10,11] On the other hand, given reports that β2-adrenergic receptors (β2-ARs) are present on Th1 T lymphocytes and antigen-presenting cells and that their activation suppresses the production of Th1 cytokines such as IFN-γ and IL-12,[12,13] β2-AR has been investigated as a potential immunomodulator in Th1 cytokine–induced autoimmune disease.[14] However, the role of β2-AR–stimulating agents on myocardial structure–mediated

Received December 14, 2005; revision received May 26, 2006; accepted June 22, 2006.

From the Department of Internal Medicine and Cardiology, Kitasato University School of Medicine, Sagamihara, Japan.

Correspondence to Dr Mototsugu Nishii, Department of Internal Medicine and Cardiology, Kitasato University School of Medicine, 1-15-1 Kitasato, Sagamihara, 228-8555 Japan. E-mail mototsugu@smz.ja-shizuoka.or.jp

Circulation is available at http://www.circulationaha.org

DOI: 10.1161/CIRCULATIONAHA.105.607903

autoimmune processes remains unknown. In this study we compared the effects of β-AR agents on EAM.

Methods

In Vivo Experiments

Induction of Rat Autoimmune Myocarditis

EAM was induced by immunizing 5-week-old female Lewis rats (Charles River Laboratory, Tsukuba, Ibaraki, Japan) with 0.25 mg of porcine cardiac myosin conjugated with complete Freund's adjuvant containing 0.25 mg of *Mycobacterium tuberculosis* H73RA (Difco, Detroit, Mich), as previously reported.[15] All experimental procedures and protocols used in this study conformed to the institutional guidelines of Kitasato University School of Medicine for the care and use of animals.

Therapeutic Protocols

Protocol I

Groups of 18 healthy animals each received intraperitoneal administration of propranolol (Sigma, St Louis, Mo) at 10 mg/kg per day as a nonselective β-AR antagonist, metoprolol at 30 mg/kg per day as a β1-selective AR antagonist (Novartis Pharmaceutical Co, Tokyo, Japan), formoterol at 22.5 μg/kg per day as a β2-selective AR agonist[16] (Yamanouchi Pharmaceutical Co, Tokyo, Japan), salbutamol at 200 μg/kg per day as a β2-selective AR agonist[13,14] (Sigma Chemical Co, St Louis, Mo), or an equal volume of phosphate-buffered saline vehicle containing 0.5% methylcellulose daily from immunization with myosin, on day 0 until euthanasia on day 21. These drugs were also administered to control groups of 8 healthy animals each without immunization with myosin for 3 weeks. Doses were selected on the basis of previous findings[17] to ensure a near-equipotent β1-AR blocking effect.

Protocol II

Groups of 12 healthy animals each were given formoterol at 22.5 μg/kg per day, salbutamol at 200 μg/kg per day, or an equal volume of vehicle by intraperitoneal administration from day 14 until day 21 after immunization with myosin.

Hemodynamic Analysis

Blood pressure (BP), heart rate (HR), and fractional shortening were determined in healthy (without myosin immunization) and diseased rats (with immunization) treated with β-AR–modulating agents or vehicle by the tail-cuff method with the use of a photoelectric tail-cuff detection system (Softron, Tokyo, Japan) and echocardiographic study (SSD-6500SV, Aloka, Tokyo, Japan) just before euthanasia on day 21. All measurements were averaged over at least 3 consecutive cardiac cycles.

Assessment of Severity of Myocarditis

All rats were killed under ether anesthesia on day 21. The ratio of heart weight to body weight (HW/BW) was calculated, and macroscopic scores were classified according to a 5-grade scoring system as previously reported.[18] The cardiac ventricles were then divided transversely into 2 sections. The ratio of the area of inflammatory infiltrates to that of the whole myocardium on a sliced half-transverse section was calculated with a microscope, as previously reported,[18] by 2 blinded observers. Interobserver and intraobserver variance was <5%.

Measurement of Cytokine Expression in Hearts

Real-time reverse transcription–polymerase chain reaction (RT-PCR) was performed to measure myocardial expression of IFN-γ or interleukin-10 (IL-10) mRNA in the other half of the hearts. Reverse transcriptase–polymerase chain reaction (RT-PCR) was performed with the use of an ABI PRISM 7700 Sequence Detection System (PE Biosystems). Positive-stranded and negative-stranded primers for mRNA amplification were ATCTGGAGGAACTGGCAAAAG-GACG and CCTTAGGCTAGATTCTGGTGACAGC for IFN-γ,[19] ACTGCTCTGTTGCCTGCTCTTACT and GAATTCAAATGCTC-CTTGATTTCT for IL-10,[19] and ACCACAGTCCATGCCATCAC and TCCACCACCCTGTTGCTGTA for glyceraldehyde phosphate dehydrogenase.[19] A standard curve was calculated with the use of the ABI PRISM 7700 System, from which the absolute copy numbers of mRNA in the samples were obtained.

In Vitro Experiments

β-AR–Modulating Agents on Myocarditogenic T-Lymphocyte Activities

A myocardiogenic CD4-positive Th1-phenotype T-lymphocyte line specific for the cardiac myosin fragment CM2 (a.a. 1539–1555)[20] was established as previously reported.[18] This T-lymphocyte line (5×10^4 per well) was cultured in triplicate supplemented with CM2 (10 μg/mL) and irradiated (5000 rad) syngeneic thymocytes as antigen-presenting cells (1×10^6 per well). Formoterol (10^{-10} to 10^{-4} mol/L), salbutamol (10^{-10} to 10^{-4} mol/L), or denopamine (10^{-10} to 10^{-4} mol/L; Tanabe Pharmaceutical Co, Tokyo, Japan) as a β1-selective AR agonist or vehicle was added to the cell-suspension culture solution, with or without ICI118,551 (10^{-8} to 10^{-6} mol/L; Tocris, Ellisville, Mo) as a β2-selective AR antagonist. After incubation, proliferation of cardiac myosin–specific T lymphocytes and levels of IFN-γ and IL-12 in each well were determined as previously described.[18] Three series of experiments were performed for each investigation.

Proliferation Assay Using Myosin-Primed Lymph Node Cells From Treated Rats

Popliteal lymph nodes were removed from Lewis rats killed 11 days after immunization with porcine cardiac myosin under daily administration of metoprolol at 30 mg/kg per day, propranolol at 10 mg/kg per day, formoterol at 22.5 μg/kg per day, salbutamol at 200 μg/kg per day, or vehicle (n=9 each). Viable mononuclear cells (5×10^4 per well) from the lymph nodes in single-cell suspension were cultured for 48 hours in triplicate with or without 10 μg/mL of cardiac myosin. Cell proliferation and levels of IFN-γ and IL-12 in each well were then determined as described previously.[18]

Intracellular cAMP Measurement

Myosin-primed lymph node cells (5×10^4 per well) from drug-treated rats (n=9 each) were cultured in triplicate with cardiac myosin as described above. Cells were pelleted by centrifugation at 1400*g* for 5 minutes followed by the addition of lysis buffer for 10 minutes. Intracellular cAMP levels were then measured with an enzyme-linked immunosorbent assay (ELISA) kit (Amersham, Piscataway, NJ).

Statistical Analysis

Data are expressed as mean±SEM. Statistical analyses were performed by 1-way ANOVA, followed by a post hoc test (Bonferroni multiple comparison test). RT-PCR analysis was performed as follows. The copy number of IFN-γ or IL-10 mRNA was normalized for GAPDH mRNA, and the myocardial expression of cytokine in each sample from EAM rats that received treatment with the β-AR agent or vehicle was then expressed as fold increase over the average level in the control group, composed of 9 EAM rats, on day 21 with no treatment. The balance of Th1 and Th2 cytokines was expressed as the ratio of IL-10 mRNA to IFN-γ mRNA: IL-10/IFN-γ. IL-10/IFN-γ level in each sample with therapy was also expressed as fold increase over that of the control group. Levels of IFN-γ, IL-10, or IL-10/IFN-γ, as well as histological and hemodynamic variables in the vehicle and control groups, were approximately equal (data not shown). To examine the effects of β-AR agents on the expression of cytokine, fold increase was compared across therapeutic groups. Probability values <0.05 were considered statistically significant.

The authors had full access to the data and take full responsibility for its integrity. All authors have read and agree to the manuscript as written.

TABLE 1. Hemodynamic Variables in Healthy Rats Treated With β-AR Agents

	Vehicle	Formoterol, 22.5 μg/kg	Salbutamol, 200 μg/kg	Metoprolol, 30 mg/kg	Propranolol, 10 mg/kg	P, ANOVA	P, Bonferroni 1 vs 2	1 vs 3	1 vs 4	1 vs 5	4 vs 5
No. of healthy rats	8	8	8	8	8						
HW/BW, %	0.48±0.02	0.52±0.03	0.50±0.02	0.50±0.02	0.49±0.03	0.88	...	...	...	...	...
Heart rate, bpm	438±6	448±4	446±6	328±8	342±6	<0.00001	0.88	0.95	<0.00001	<0.00001	0.20
SBP, mm Hg	133±2	139±4	142±4	111±3	113±4	<0.00001	0.18	0.06	<0.00001	<0.00001	2.26
DBP, mm Hg	88±3	82±3	90±2	73±2	74±2	<0.00001	0.09	0.89	<0.00001	<0.00001	2.11
Fractional shortening, %	76±3	79±3	79±3	76±3	75±4	0.68	...	...	...	...	...

Values are mean±SEM. 1 indicates vehicle group; 2, formoterol group; 3, salbutamol group; 4, metoprolol group; 5, propranolol group; SBP, systolic blood pressure; and DBP, diastolic blood pressure. One-way ANOVA was used to test for differences among groups, and, when appropriate, Bonferroni multiple comparison test was performed to test difference between 2 groups.

Results

Hemodynamics in Healthy Rats Treated With β-AR Agents

HR and BP were significantly decreased in the rats of the 2 β-AR antagonist groups compared with the vehicle group, with no significant difference between them. In contrast, no change in hemodynamic variables was seen in the formoterol or salbutamol groups (Table 1).

Administration of β-AR Agents Starting on Day 0

Mortality

Four diseased rats treated with vehicle or metoprolol (mortality: 4/18, 22%) died between days 19 and 21, and 8 diseased rats treated with propranolol (8/18, 44%) died between days 15 and 21. However, all diseased rats treated with the β2-AR agonists (0/18, 0%) survived until day 21.

Hemodynamics

Compared with the vehicle group, BP, HR, and fractional shortening were significantly decreased in the β-AR antagonist groups, whereas fractional shortening and BP were significantly increased with a decrease of HR in the β2-AR agonist groups. No significant differences in hemodynamic variables were seen between the β-AR antagonist groups (Table 2).

Severity of Disease

Macroscopic score, HW/BW, and area of cellular infiltration into the myocardium were significantly reduced in the 2 β2-AR agonist groups, indicating a significantly reduced severity of disease. In contrast, the propranolol but not the metoprolol group showed a significantly increased severity of disease compared with the vehicle group (Figure 1, Table 2).

Cytokine Profiles

Compared with the vehicle group, levels of IFN-γ and IL-10 mRNA in the myocardium were significantly increased in the propranolol but not in the metoprolol group. In contrast, levels were decreased in both the formoterol and salbutamol groups. However, IL-10/IFN-γ was significantly decreased in the propranolol group but increased in the 2 β2-AR agonist groups compared with the vehicle group (Table 2).

Administration of β2-AR Agonist From Day 14 After Immunization

Mortality

Three diseased rats treated with the vehicle (mortality: 3/12, 25%) died between days 19 and 21, whereas all diseased rats treated with the β2-AR agonists (0/12, 0%) survived until day 21.

TABLE 2. Histological and Hemodynamic Variables and Cytokine Profiles in EAM Rats Treated From Day 0

	Vehicle	Formoterol, 22.5 μg/kg	Salbutamol, 200 μg/kg	Metoprolol, 30 mg/kg	Propranolol, 10 mg/kg	P, ANOVA	P, Bonferroni 1 vs 2	1 vs 3	1 vs 4	1 vs 5	4 vs 5
No. of EAM rats	14	18	18	14	10	...	...	...	...	...	...
Macroscopic score	2.8±0.1	1.4±0.1	1.2±0.1	2.6±0.1	3.6±0.2	<0.00001	<0.00001	<0.00001	0.39	<0.00001	<0.00001
HW/BW, %	0.82±0.02	0.56±0.01	0.51±0.01	0.84±0.02	1.13±0.02	<0.00001	<0.00001	<0.00001	0.81	<0.00001	<0.00001
Cellular infiltration area, %	68.6±2.1	32.4±2.0	28.6±1.6	64.9±2.5	89.1±3.2	<0.00001	<0.00001	<0.00001	0.49	<0.00001	<0.00001
Heart rate, bpm	476±5	458±5	456±4	426±5	436±5	<0.00001	0.0031	0.00044	<0.00001	<0.00001	0.21
SBP, mm Hg	120±3	132±2	136±3	90±3	86±2	<0.00001	0.00001	<0.00001	<0.00001	<0.00001	0.47
DBP, mm Hg	82±2	80±2	88±2	60±2	58±3	<0.00001	0.89	0.17	<0.00001	<0.00001	0.94
Fractional shortening, %	46±3	66±2	70±3	31±2	26±3	<0.00001	<0.00001	<0.00001	<0.00001	<0.00001	0.25
IFN-γ, fold increase	0.99±0.02	0.46±0.02	0.42±0.02	0.93±0.02	3.82±0.21	<0.00001	<0.00001	<0.00001	0.19	<0.00001	<0.00001
IL-10, fold increase	0.98±0.01	0.88±0.02	0.83±0.02	0.95±0.01	1.63±0.02	<0.00001	<0.00001	<0.00001	0.28	<0.00001	<0.00001
IL-10/IFN-γ, fold increase	0.99±0.02	1.83±0.04	1.98±0.04	1.02±0.02	0.43±0.01	<0.00001	<0.00001	<0.00001	2.12	<0.00001	<0.00001

Values are mean±SEM. 1 indicates vehicle group; 2, formoterol group; 3, salbutamol group; 4, metoprolol group; 5, propranolol group; SBP, systolic blood pressure; and DBP, diastolic blood pressure. Level of IFN-γ, IL-10, or IL-10/IFN-γ in each group is represented as mean±SEM for fold increases over each average level in the control group.

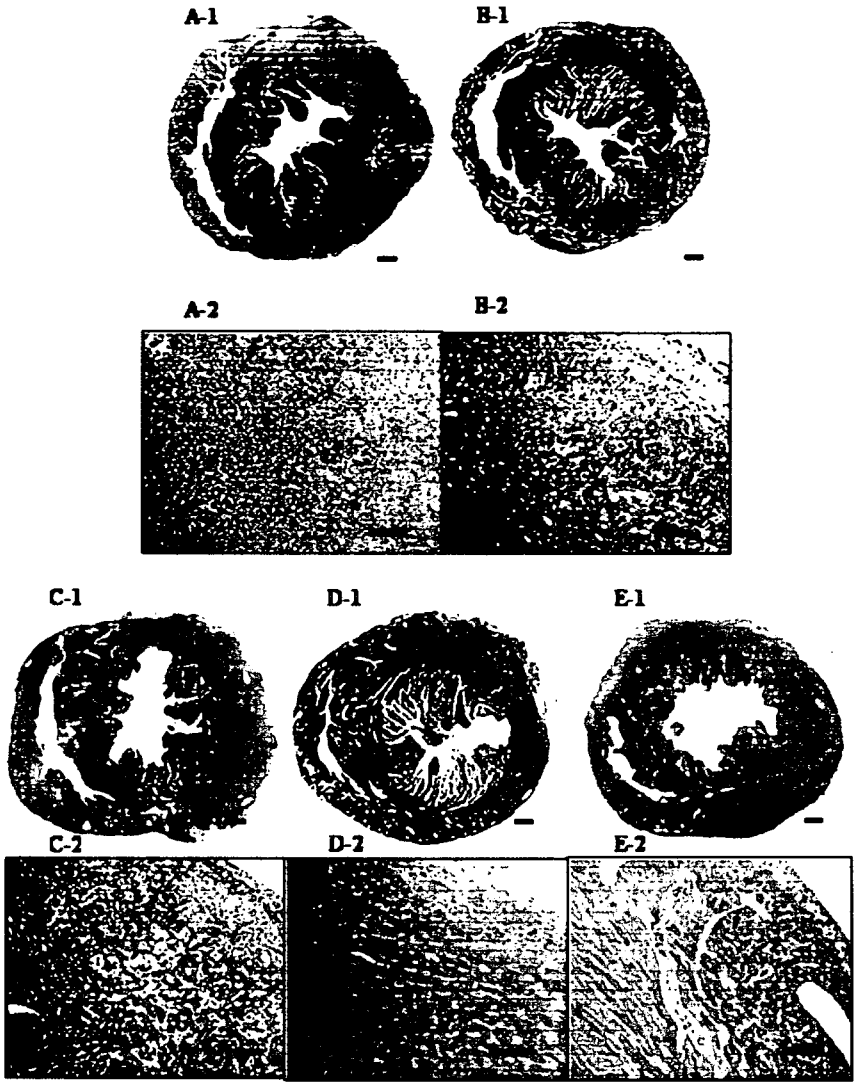

Figure 1. Histological findings in EAM hearts on day 21 of in vivo administration of β-AR agents. Administration of propranolol at 10 mg/kg (A) facilitated interstitial cellular infiltration compared with that of metoprolol at 30 mg/kg (B) or vehicle (C). Conversely, administration of either formoterol at 22.5 μg/kg (D) or salbutamol at 200 μg/kg ameliorated interstitial cellular infiltration (E). Bars=1 mm or 250 μm (thick, for ×1; thin, for ×40, respectively).

Hemodynamics

Among hemodynamic variables, significant increases in fractional shortening and systolic blood pressure were seen, with a significant decrease in heart rate in the formoterol and salbutamol groups compared with the vehicle group (Table 3).

Severity of Disease

Disease severity as indicated by macroscopic score, HW/BW, and area of cellular infiltration into the myocardium was significantly decreased in the formoterol and salbutamol groups compared with the vehicle group (Table 3). These macroscopic findings were reflected in microscopic findings, which included interstitial cellular infiltration and destruction of myocardial fibers (Figure 2).

Cytokine Profiles

Compared with levels in the vehicle group, myocardial mRNA levels of IFN-γ and IL-10 were significantly decreased in both the formoterol group and salbutamol group. In contrast, myocardial IL-10/IFN-γ mRNA levels were significantly increased in the β2-AR agonist groups compared with the vehicle group (Table 3).

Myocardiogenic T Lymphocytes and β-AR Stimulation

Formoterol as well as salbutamol strongly and dose-dependently suppressed cardiac myosin-specific T-lymphocyte proliferation and IL-12 production by antigen-presenting cells and IFN-γ production by T lymphocytes, whereas denopamine only slightly suppressed cardiac myosin-specific T-lymphocyte activity (Figure 3). ICI118,551 reversed these inhibitory effects of formoterol or salbutamol (Figure 4).

Influence of In Vivo Administration of β-AR Agents on Lymph Node Cell Activity

The proliferation of cardiac myosin-primed lymph node cells from treated EAM rats and their production of IL-12 and IFN-γ were significantly decreased in both the formoterol group (6399±297 cpm, 76±4.9 pg/mL, 3480±145 pg/mL, respectively; each $P<0.00001$ versus the vehicle group) and the salbutamol group (6140±295 cpm, 61±4.5 pg/mL, 3012±189 pg/mL, respectively; each $P<0.00001$ versus the vehicle group) compared with the vehicle group (13283±309 cpm, 173±12 pg/mL, 12913±429 pg/mL, respectively). Conversely, cell proliferation and cytokine production were

TABLE 3. Histological and Hemodynamic Variables and Cytokine Profiles in EAM Rats Treated From Day 14

	Vehicle	Formoterol, 22.5 μg/kg	Salbutamol, 200 μg/kg	P, ANOVA	P, Bonferroni 1 vs 2	1 vs 3	2 vs 3
No. of EAM rats	9	12	12				
Macroscopic score	2.9±0.1	2.2±0.1	2.0±0.1	0.00044	0.00005	<0.00001	0.62
HW/BW, %	0.82±0.03	0.72±0.02	0.68±0.02	<0.00001	<0.00001	<0.00001	0.06
Cellular infiltration area, %	70.6±2.7	48.4±1.3	42.4±2.0	<0.00001	<0.00001	<0.00001	0.0004
Heart rate, bpm	478±2	468±3	466±2	0.031	0.0079	0.0013	0.95
SBP, mm Hg	120±2	128±2	126±2	0.025	0.00078	0.029	0.32
Fractional shortening, %	44±2	56±2	58±2	<0.00001	<0.000001	<0.000001	0.70
IFN-γ, fold increase	1.01±0.03	0.44±0.02	0.41±0.01	<0.00001	<0.00001	<0.00001	0.24
IL-10, fold increase	1.02±0.03	0.89±0.02	0.84±0.02	0.00024	0.00002	<0.00001	0.08
IL-10/IFN-γ, fold increase	1.01±0.03	2.01±0.05	2.05±0.04	<0.00001	<0.00001	<0.00001	0.99

Values are mean±SEM. 1 indicates vehicle group; 2, formoterol group; 3, salbutamol group; and SBP, systolic blood pressure. Level of IFN-γ, IL-10, or IL-10/IFN-γ in each group is represented as mean±SEM for fold increases over each average level in the control group.

significantly increased in the propranolol group (28233±527 cpm, 402±24 pg/mL, 44022±1408 pg/mL, respectively; each $P<0.00001$ versus the vehicle group) but not in the metoprolol group (12388±253 cpm, $P=0.08$; 157±13 pg/mL, $P=0.96$; 13939±392 pg/mL, $P=0.58$; respectively) (Figure 5). Cell proliferation and cytokine expression were not observed in any culture without cardiac myosin (300±14 cpm).

Administration of formoterol and salbutamol increased intracellular cAMP levels in myosin-primed lymph node cells compared with vehicle (188±12, 179±9, versus 39±2 fmol, respectively; each $P<0.00001$), whereas that of propranolol decreased cAMP levels (11±0.8 fmol; $P=0.00007$ versus the vehicle group). Administration of metoprolol did not affect intracellular cAMP level (36±1 fmol; $P=2.39$ versus the vehicle group) (Figure 5).

Discussion

The role of β-adrenergic stimulation on myocarditis has been investigated. It has been shown that the β1-AR agonist denopamine prolongs survival in mice with viral myocarditis.[21] However, other recent reports demonstrated that metoprolol, a β1-selective AR antagonist, did not affect disease severity and mortality in rats with autoimmune myocarditis[22] and mice with viral myocarditis,[23] suggesting that β1-AR has only a weak modulatory effect on the development of myocarditis. Thus, the protective effect of denopamine on myocarditis may result from an improvement in hemodynamic deterioration via its positive inotropic effect rather than from any other effect. On the other hand, these reports also indicated the immunomodulatory potential on myocarditis of carvedilol, which has β-AR–blocking and antioxidative effects,[22,23] and indicated that this effect was explained mainly by its antioxidative effect. However, the role of β2-AR stimulation on myocarditis remains uncertain.

Wide use of β2-selective AR–stimulating agents such as formoterol and salbutamol has been restricted to bronchodilation in patients with asthma. Recently, however, interest in these agents was renewed for their potential immunomodulatory role in Th1 cytokine–induced autoimmune disease. Catecholamines and several adrenergic agonists have been shown to influence the production of Th1 cytokines, and β2-AR is involved in this mechanism.[12,13] Furthermore, intraperitoneal administration of salbutamol, a β2-selective AR agonist, suppressed Th1 cytokine–induced autoimmune arthritis via β2-AR in vivo.[14] In the present study, the 2 β2-selective AR agonists formoterol and salbutamol did not affect hemodynamics in healthy rats (Table 1) but ameliorated Th1 cytokine–induced EAM[10,11] on day 21 (Table 2) and reduced mortality. Furthermore, treatment with propranolol but not metoprolol exacerbated EAM on day 21 and increased mortality, despite showing equivalent hemodynamic effects (Table 2). The different effect of the 2 β-blockers according to β-AR selectivity supports the existence of an immunomodulatory role of β2-AR in the development of EAM. Together, the present results indicate that β2-AR–stimulating agents can ameliorate the development of EAM via β2-AR.

In myocarditis, the autoimmune process leads to myocardial inflammation and injury via the effect of activated Th1 T lymphocytes specific for cardiac myosin.[10,24] Th1 cytokines such as IL-12 and IFN-γ promote this process.[10] It has been demonstrated that β2-AR stimulation inhibits the production of IFN-γ and IL-12 in vitro.[12,13] Furthermore, inhibition of antigen-specific T-cell proliferation was reported to be a therapeutic strategy for retarding the development of myocarditis.[25] The protective effect on EAM of the 2 β2-selective AR agonists seen here can therefore be explained by the idea that β2-AR stimulation attenuates cardiac myosin–specific Th1 T-lymphocyte proliferation by suppressing the production of Th1 cytokines. However, the suppressive effect of β2-AR stimulation on cardiac myosin–specific Th1 T-lymphocyte activity has not been elucidated.

To clarify this point, we used in vitro experimental systems using the immunodominant myosin peptide–specific CD4-positive Th1 T-lymphocyte line, the transfer of which induces EAM,[18] and ex vivo experimental systems using cardiac myosin–primed lymph nodes from β-AR agent–treated rats. The myocarditogenic Th1 T-lymphocyte line was stimulated

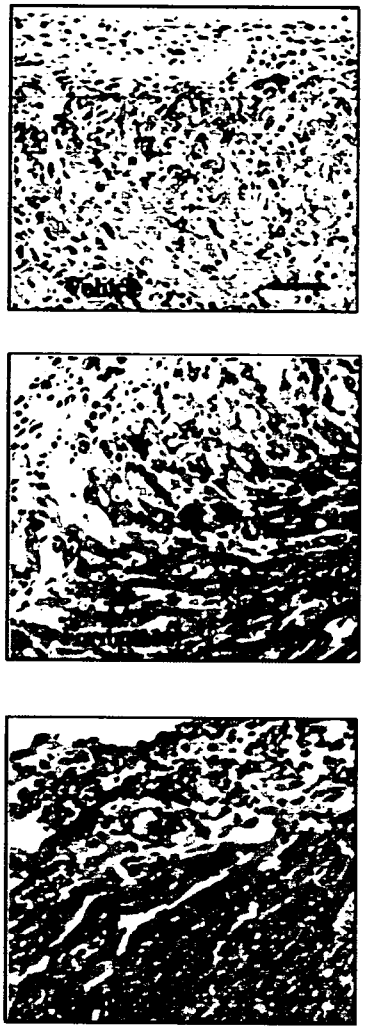

Figure 2. Microscopic findings in EAM rats treated with formoterol at 22.5 μg/kg, salbutamol at 200 μg/kg, or vehicle from days 14 to 21. β2-AR agonists reduced interstitial cellular infiltration and destruction of myocardial fibers compared with the vehicle. Bars=250 μm (thin, for ×100).

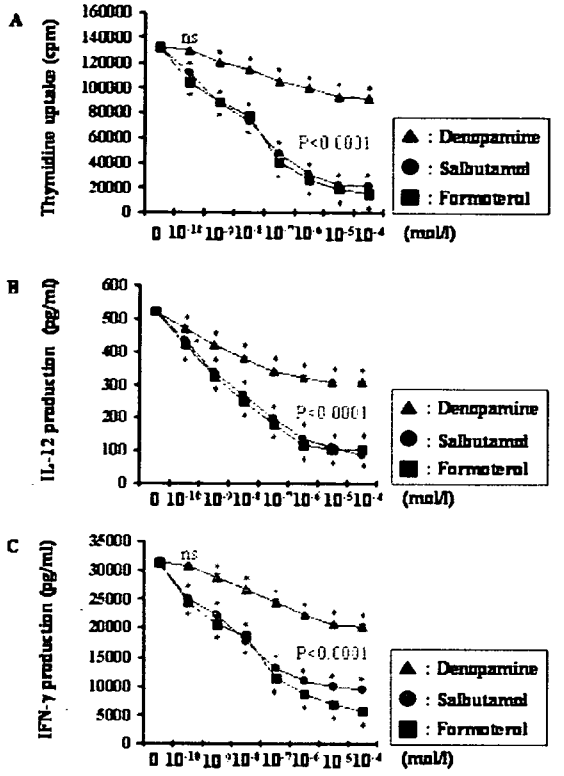

Figure 3. Effects of β-AR agonists on myocarditogenic T lymphocytes stimulated by specific antigen and antigen-presenting cells. Cell proliferation (A) and production of IL-12 (B) and IFN-γ (C) in the culture supernatant were determined by ^{3}H-thymidine uptake and an ELISA kit. Three series of experiments were performed for each investigation. Error bars represent SEM. β-AR agonists decreased cell proliferation and production of IL-12 and IFN-γ (*P<0.00001 vs culture with vehicle only), and inhibitory effects by formoterol and salbutamol were very much stronger compared with denopamine in each concentration (P<0.0001).

with antigen-presenting cells and the specific antigen to emulate the priming step of EAM in vivo. Both formoterol and salbutamol reduced cardiac myosin–specific T-lymphocyte proliferation by suppressing the production of IL-12 and IFN-γ (Figure 3). ICI118,551, a β2-selective AR antagonist, but not metoprolol (data not shown), completely reversed the inhibitory effects of formoterol and salbutamol (Figure 4). Along with the difference in myosin-primed lymph node cell proliferation among formoterol-treated, salbutamol-treated, propranolol-treated, metoprolol-treated, and vehicle-treated rats (Figure 5), these results suggested that β2-AR–stimulating agents ameliorated the induction of EAM by attenuating cardiac myosin–specific Th1 T-lymphocyte proliferation in the lymphoid organs associated with the suppression of Th1 cytokines via β2-AR stimulation. Previous reports have demonstrated that β2-AR is present on Th1 T lymphocytes and antigen-presenting cells and that its activation inhibits their production of Th1 cytokines by increasing intracellular cAMP levels.[12,13] In our ex vivo experiment, β2-AR stimulation inhibited myosin-primed lymph node cell activity adversely, in parallel with increasing intracellular cAMP levels (Figure 5). Thus, the inhibitory effect of β2-AR stimulation on Th1 T lymphocytes specific for the cardiac myosin–mediated immune response identified here may have contributed to the activation of the β2-AR–cAMP signaling pathway on Th1 T lymphocytes and antigen-presenting cells.

An imbalance in Th1 and Th2 cytokines modulates the pathogenesis of EAM,[11] and the Th2 cytokine IL-10 plays a protective role in the development of EAM.[26] Previous reports showed that shifting the immune response toward the Th2 pattern prevented the development of EAM.[10,27] Thus, we examined the production of the Th1 cytokine IFN-γ and Th2 cytokine IL-10 in the heart. Administration of either formoterol or salbutamol, but not of propranolol, starting on day 0 reduced myocardial IFN-γ expression on day 21 compared with the vehicle group. The influences of drugs on myocardial IL-10 expression showed a similar pattern, although to a lesser degree, which is in part associated with the interaction of IL-10 and IFN-γ during the course of their production. However, myocardial IL-10/IFN-γ mRNA expression was significantly increased in the 2 β2-AR agonist

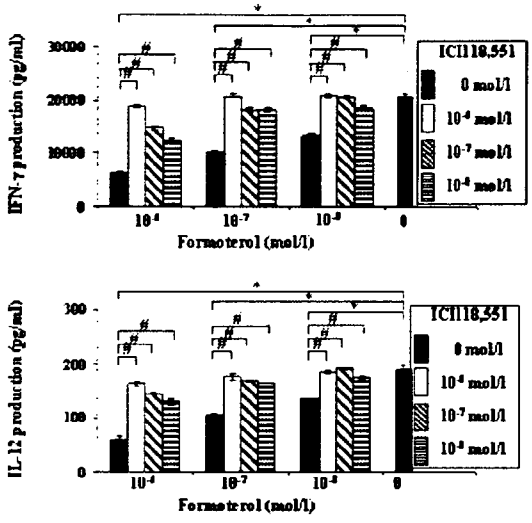

Figure 4. ICI118,551 reversed the inhibitory effect of β2-AR stimulation on the production of Th1-cytokines. Levels of IL-12 and IFN-γ in the culture supernatant were determined by an ELISA kit. Three series of experiments were performed for each investigation. Error bars represent SEM. *$P<0.00001$ vs culture with the vehicle only; #$P<0.00001$ vs each concentration of formoterol without ICI118,551.

groups, whereas it was significantly decreased in the propranolol group (Table 2). This finding suggests that β2-AR stimulation shifts the myocardial Th1/Th2 cytokine balance toward Th2 cytokines and that this effect in part contributes to modulating the development of EAM by β2-AR–stimulating agents.

Not only extremely suppressed myocardial IFN-γ expression by β2-AR stimulation but also in part enhanced IL-10 expression by it may contribute to alteration of the myocardial Th1/Th2 cytokine balance in vivo. Myocardial inflammation in EAM mainly involves macrophages and CD4-positive Th1 T lymphocytes, and the dominance of these cells is a constant finding at lesion sites and throughout the course of the disease.[28] The enhancement of IL-10 production in inflammatory cells such as monocytes, macrophages, and dendritic cells via β2-AR stimulation has been reported.[29,30]

Propranolol enhanced disease severity in the present study. However, recent studies in the BALB/c mouse model of viral myocarditis found that propranolol exerts a protective effect against myocarditis.[31] This difference may be explained in part by the promotion of a Th1 response in this infectious model, which clears the virus.[23,31]

In the present study, our intervention with β2-AR–stimulating agents was done in a later phase of EAM to examine their effect on established myocardial inflammation. Formoterol and salbutamol significantly reduced the severity and mortality of myocarditis (Table 3) and significantly increased myocardial IL-10/IFN-γ mRNA levels on day 21 compared with the vehicle (Table 3). β2-AR–stimulating agents also ameliorated established myocardial inflammation, and this beneficial effect was in part associated with an alteration in the myocardial Th1/Th2 cytokine balance. Given that human myocarditis is usually diagnosed after disease onset, this result has important implications for clinical treatment.

Chronic β-AR stimulation in heart failure induces myocardial apoptosis and thereby induces progressive myocardial remodeling.[32] However, recent reports have demonstrated opposing effects of β1- and β2-AR stimulation on cardiac myocytes. In rat cardiomyocytes, β1-AR stimulation induces apoptosis via a cAMP-dependent mechanism, whereas β2-AR stimulation inhibits this process.[33] A transgenic mice model overexpressing β1-AR developed dilated cardiomyop-

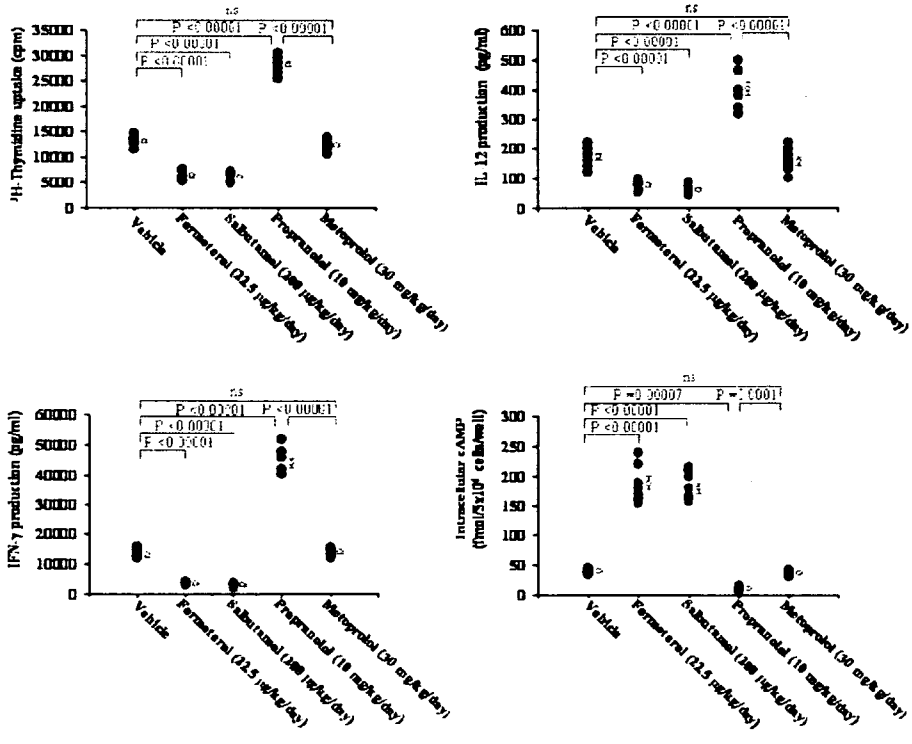

Figure 5. The proliferation of T lymphocytes and levels of IL-12, IFN-γ, and intracellular cAMP in cardiac myosin–primed lymph nodes from EAM rats treated with β-AR agent or vehicle. Cell proliferation, levels of Th1-cytokines, and levels of intracellular cAMP were determined by measuring radioactivity of incorporated ^{3}H-thymidine and an ELISA kit. Each group contained 9 rats. Closed circle indicates individual data; open circle and error bar, mean±SEM for each group. No significant difference was shown in comparisons of metoprolol and vehicle groups.

athy along with hemodynamic deterioration, whereas those overexpressing β2-AR did not.[34,35] In the present study, treatment with β2-AR agonists at doses that did not affect hemodynamic variables in healthy rats (Table 1) throughout the acute phase at least improved cardiac contractility in EAM rats (Table 2), and decreasing HR compared with the vehicle group (Table 2) may reflect an improvement of cardiac function. The new immunomodulatory effect of β2-AR stimulation identified here also contributed to this effect. β2-AR–stimulating agents thus may represent the preferred therapy for inflammatory myocardial conditions with hemodynamic deterioration derived from autoimmune processes.

Conclusions

To our knowledge, this study is the first to report that β2-AR–stimulating agents ameliorate the development of EAM by reducing cardiac myosin–specific T-cell activity in the lymphoid organs, which plays an important role in the initiation of myocarditis, and by altering the imbalance between Th1 and Th2 cytokines. These agents also ameliorate established myocardial inflammation. These findings indicate that β2-AR stimulation is a major immunomodulatory factor in the development of EAM. The potential of β2-AR–stimulating agents as new therapeutic drugs for the treatment of myocarditis requires further investigation.

Acknowledgments

We thank Toshie Hashizume and Chiaki Notoya for their outstanding technical assistance.

Sources of Funding

This study was supported by a grant-in-aid for scientific research from the Postgraduate Research Project at Kitasato University and a grant for scientific research from the Ministry of Education, Science, and Culture of Japan (No. 20311954).

Disclosures

None.

References

1. Nishii M, Inomata T, Takehana H, Takeuchi I, Nakano H, Koitabashi T, Nakahata J, Aoyama N, Izumi T. Serum levels of interleukin-10 on admission as a prognostic predictor of human fulminant myocarditis. *J Am Coll Cardiol.* 2004;44:1292–1297.
2. Hühl U, Noutsias M, Seeberg B, Schultheiss HP. Immunohistochemical evidence for a chronic intramyocardial inflammatory process in dilated cardiomyopathy. *Heart.* 1996;75:295–300.
3. Jin O, Sole MJ, Butany JW, Chia WK, McLaughlin PR, Liu P, Liew CC. Detection of enterovirus RNA in myocardial biopsies from patients with myocarditis and cardiomyopathy using gene amplification by polymerase chain reaction. *Circulation.* 1990;82:8–16.
4. Kodama M, Hanawa H, Saeki M, Hosono H, Inomata T, Suzuki K, Shibata A. Rat dilated cardiomyopathy after autoimmune giant cell myocarditis. *Circ Res.* 1994;75:278–284.
5. Nakamura H, Yamamura T, Umemoto S, Fukuta S, Shioi T, Matsumori A, Sasayama S, Matsuzaki M. Autoimmune response in chronic ongoing myocarditis demonstrated by heterotopic cardiac transplantation in mice. *Circulation.* 1996;94:3348–3354.
6. Rose NR, Hill SL. The pathogenesis of postinfectious myocarditis. *Clin Immunol Immunopathol.* 1996;80:S92–S99.
7. Hubes SA, Lodge PA. Coxsackievirus B3 myocarditis in BALB/c mice: evidence for autoimmunity to myocyte antigens. *Am J Pathol.* 1984;116:21–29.
8. Lauer B, Padberg K, Schultheiss HP, Strauer BE. Autoantibodies against cardiac myosin in patients with myocarditis and dilated cardiomyopathy. *Z Kardiol.* 1995;84:301–310.
9. Maisch B, Deeg P, Liebau G, Kochsiek K. Diagnostic relevance of humoral and cytotoxic immune reactions in primary and secondary dilated cardiomyopathy. *Am J Cardiol.* 1983;52:1072–1078.
10. Okura Y, Takeda K, Honda S, Hanawa H, Watanabe H, Kodama M, Izumi T, Aizawa Y, Seki S, Abo T. Recombinant murine interleukin-12 facilitates induction of cardiac myosin-specific type 1 helper T cells in rats. *Circ Res.* 1998;82:1035–1042.
11. Okura Y, Yamamoto T, Goto S, Inomata T, Hirono S, Hanawa H, Feng L, Wilson CB, Kihara I, Izumi T, Shibata A, Aizawa Y, Seki S, Abo T. Characterization of cytokine and iNOS mRNA expression in situ during the course of experimental autoimmune myocarditis in rats. *J Mol Cell Cardiol.* 1997;29:491–502.
12. Borger P, Hoekstra Y, Esselink MT, Postma DS, Zaagsma J, Vellenga E, Kauffman HF. Beta-adrenoceptor-mediated inhibition of IFN-gamma, IL-3, and GM-CSF mRNA accumulation in activated human T lymphocytes is solely mediated by the beta2-adrenoceptor subtype. *Am J Respir Cell Mol Biol.* 1998;19:400–407.
13. Panina-Bordignon P, Mazzeo D, Lucia PD, D'Ambrosio D, Lang R, Fabbri L, Self C, Sinigaglia F. Beta2-agonists prevent Th1 development by selective inhibition of interleukin-12. *J Clin Invest.* 1997;100:1513–1519.
14. Malfait AM, Malik AS, Marinova-Mutafchieva L, Butler DM, Maini RN, Feldmann M. The beta2-adrenergic agonist salbutamol is a potent suppressor of established collagen-induced arthritis: mechanisms of action. *J Immunol.* 1999;162:6278–6283.
15. Inomata T, Hanawa H, Miyanishi T, Yajima E, Nakayama S, Maita T, Kodama M, Izumi T, Shibata A, Abo T. Localization of porcine cardiac myosin epitopes that induce experimental autoimmune myocarditis. *Circ Res.* 1995;76:726–733.
16. van der Molen T, Sears MR, de Graaff CS, Postma DS, Meyboom-de Jong B, for the Canadian and Dutch Formoterol Investigators. Quality of life during formoterol treatment: comparison between asthma-specific and generic questionnaires. *Eur Respir J.* 1998;12:30–34.
17. Sponer G, Bartsch W, Strein K, Muller-Beckmann B, Bohm E. Pharmacological profile of carvedilol as a beta-blocking agent with vasodilating and hypertensive properties. *J Cardiovasc Pharmacol.* 1987;9:317–327.
18. Takehana H, Inomata T, Niwano H, Nishii M, Matsuda C, Kohno K, Machida Y, Izumi T. Immunomodulatory effect of pentoxifyline in suppressing experimental autoimmune myocarditis. *Jpn Circ J.* 2002;66:499–504.
19. Hanawa H, Abe S, Hayashi M, Yoshida T, Yoshida K, Shiono T, Fuse K, Ito M, Tachikawa H, Kashimura T, Okura Y, Kato K, Kodama M, Maruyama S, Yamamoto T, Aizawa Y. Time course of gene expression in rat experimental autoimmune myocarditis. *Clin Sci.* 2002;103:623–632.
20. Wegmann KW, Zhao W, Griffin AC, Hickey WF. Identification of myocarditogenic peptides derived from cardiac myosin capable of inducing experimental allergic myocarditis in the Lewis rat. *J Immunol.* 1994;153:892–900.
21. Nishio R, Matsumori A, Shioi T, Wang W, Yamada T, Ono K, Sasayama S. Denopamine, a beta1-adrenergic agonist, prolongs survival in a murine model of congestive heart failure induced by viral myocarditis: suppression of tumor necrosis factor-alpha production in the heart. *J Am Coll Cardiol.* 1998;32:808–815.
22. Yuan Z, Shioji K, Kihara Y, Takenaka H, Onozawa Y, Kishimoto C. Cardioprotective effects of carvedilol on acute autoimmune myocarditis: anti-inflammatory effects associated with antioxidant property. *Am J Physiol.* 2004;286:83–90.
23. Nishio R, Shioi T, Sasayama S, Matsumori A. Carvedilol increases the production of interleukin-12 and interferon-gamma and improves the survival of mice infected with the encephalomyocarditis virus. *J Am Coll Cardiol.* 2003;41:340–345.
24. Kodama M, Matsumoto Y, Fujiwara M. In vivo lymphocyte-mediated myocardial injuries demonstrated by adoptive transfer of experimental autoimmune myocarditis. *Circulation.* 1992;85:1918–1926.
25. Futamatsu H, Suzuki J, Kosuge H, Yokoseki O, Kamada M, Ito H, Inobe M, Isobe M, Uede T. Attenuation of experimental autoimmune myocarditis by blocking activated T cells through inducible costimulatory molecule pathway. *Cardiovasc Res.* 2003;59:95–104.
26. Watanabe K, Nakazawa M, Fuse K, Hanawa H, Kodama M, Aizawa Y, Ohnuki T, Gejyo F, Maruyama H, Miyazaki J. Protection against auto-

immune myocarditis by gene transfer of interleukin-10 by electroporation. *Circulation.* 2001;104:1098–1100.
27. Futamatsu H, Suzuki J, Mizuno S, Koga N, Adachi S, Kosuge H, Maejima Y, Hirao K, Nakamura T, Isobe M. Hepatocyte growth factor ameliorates the progression of experimental autoimmune myocarditis: a potential role for induction of T helper 2 cytokines. *Circ Res.* 2005;96:823–830.
28. Kodama M, Zhang S, Hanawa H, Shibata A. Immunohistochemical characterization of infiltrating mononuclear cells in the rat heart with experimental autoimmune giant cell myocarditis. *Clin Exp Immunol.* 1992;90:330–335.
29. Kavelaars A, van de Pol M, Zijlstra J, Heijnen CJ. Beta2-adrenergic activation enhances interleukin-8 production by human monocytes. *J Neuroimmunol.* 1997;77:211–216.
30. van der Poll T, Coyle SM, Barbosa K, Braxton CC, Lowry SF. Epinephrine inhibits tumor necrosis factor-alpha and potentiates interleukin-10 production during human endotoxemia. *J Clin Invest.* 1996;97:713–719.
31. Wang JF, Meissner A, Malek S, Chen Y, Ke Q, Zhang J, Chu V, Hampton TG, Crumpacker CS, Abelmann WH, Amende I, Morgan JP. Propranolol ameliorates and epinephrine exacerbates progression of acute and chronic viral myocarditis. *Am J Physiol.* 2005;289:1577–1583.
32. Bristow MR. Beta-adrenergic receptor blockade in chronic heart failure. *Circulation.* 2000;101:558–569.
33. Communal C, Singh K, Sawyer DB, Colucci WS. Opposing effects of beta1- and beta2-adrenergic receptors on cardiac myocyte apoptosis: role of a pertussis toxin-sensitive G protein. *Circulation.* 1999;100:2210–2212.
34. Bisognano JD, Weinberger HD, Bohlmeyer TJ, Pende A, Raynolds MV, Sastravaha A, Roden R, Asano K, Blaxall BC, Wu SC, Communal C, Singh K, Colucci WS, Bristow MR, Port DJ. Myocardial-directed overexpression of the human beta1-adrenergic receptor in transgenic mice. *J Mol Cell Cardiol.* 2000;32:817–830.
35. Rockman HA, Hamilton RA, Jones LR, Milano CA, Mao L, Lefkowitz RJ. Enhanced myocardial relaxation in vivo in transgenic mice overexpressing the beta2-adrenergic receptor is associated with reduced phospholamban protein. *J Clin Invest.* 1996;97:1618–1623.

CLINICAL PERSPECTIVE

We present a compelling case for evaluating β2-adrenergic agonists in patients with myocarditic heart failure. Differences among in vivo therapies with β2-adrenergic agonists, propranolol as a nonselective β-adrenergic antagonist, and metoprolol as a β1-selective adrenergic antagonist in rat experimental autoimmune myocarditis (EAM) produced by immunization with cardiac myosin demonstrated that β2-adrenergic agonists modulate the development of EAM via β2-adrenergic stimulation. This effect was associated with modulating myocarditogenic Th1 T lymphocytes specific for cardiac myosin–mediated immune response in the lymphoid organs and shifting the imbalance of the Th1 cytokine and Th2 cytokine pattern toward the Th2 cytokine pattern in the myocardium, which was contributed to the suppression of Th1 cytokine production by β2-adrenergic stimulation. Therapy with β2-adrenergic agonists furthermore suppressed not only the induction of myocarditis but also established myocardial inflammation. It contributed to the improvement of hemodynamics and mortality in EAM. Taken together, these findings indicate the new role of the β2-adrenergic agonist as an immunomodulator in the development of EAM and may provide a novel approach for therapy in patients suffering from inflammatory myocardial conditions with hemodynamic deterioration, particularly those derived from autoimmune processes. Interest in β2-adrenergic agonists, which has been restricted to bronchodilators, should be renewed because of their potential as an immunomodulatory and therapeutic agent in myocardial inflammatory disease complicated by heart failure.

European Heart Journal (2005) 26, 2698–2705
doi:10.1093/eurheartj/ehi492

Clinical research

Increased gene expression of collagen Types I and III is inhibited by β-receptor blockade in patients with dilated cardiomyopathy

Junsho Shigeyama[1], Yoshio Yasumura[1], Aiji Sakamoto[2], Yoshio Ishida[3], Tatsuya Fukutomi[4], Makoto Itoh[4], Kunio Miyatake[1], and Masafumi Kitakaze[1]*

[1] *Division of Cardiology, Department of Medicine, National Cardiovascular Center, 5-7-1 Fujishirodai, Suita, Osaka 565-8565, Japan;* [2] *Division of Biotechnology, National Cardiovascular Center Research Institute, Osaka, Japan;* [3] *Division of Radiology, National Cardiovascular Center, Osaka, Japan; and* [4] *Department of Internal Medicine and Bioregulation, Nagoya City University Graduate School of Medical Sciences, Aichi, Japan*

Received 3 January 2005; revised 10 August 2005; accepted 18 August 2005; online publish-ahead-of-print 4 October 2005

KEYWORDS
Collagen synthesis;
β-Blocker;
Myocardial gene expression;
Heart failure;
Dilated cardiomyopathy

Aims To elucidate the cellular mechanisms of cardioprotection of β-blockers in patients with heart failure, we investigated the effects of β-blockers on collagen synthesis in patients with dilated cardiomyopathy (DCM).

Methods and results We examined the gene expression before and 4 months after the administration of a β-blocker in 17 DCM patients. The messenger ribonucleic acid expression of collagen Types I and III (Col I and III) and transforming growth factor-β_1 (TGF-β_1) of right ventricular tissues obtained by the endomyocardial biopsy were assessed by quantitative reverse transcriptase-polymerase chain reaction. Cardiac sympathetic nerve activity was assessed by the washout rate (WR) of ^{123}I-metaiodobenzylguanidine from the heart. Left ventricular ejection fraction (21 ± 7 vs. $35 \pm 9\%$) and WR (53 ± 14 vs. $42 \pm 13\%$) improved significantly. Before the β-blocker treatment, the expressions of both Col I ($r = 0.560$, $P = 0.041$) and Col III ($r = 0.630$, $P = 0.008$) genes were correlated with WR. The expression levels of both Col I (1.08 ± 0.72 vs. 0.65 ± 0.26, $P = 0.024$) and Col III (2.06 ± 1.81 vs. 1.05 ± 0.74, $P = 0.018$) were reduced by a β-blocker. Changes in TGF-β_1 correlated with those in WR ($r = 0.606$, $P = 0.002$).

Conclusion β-Blockers are considered to inhibit the expression of collagen-related genes in DCM, which seems to be mediated by TGF-β_1.

Introduction

β-Blockers that decrease the mortality and morbidity in patients with heart failure are recognized to improve systolic ventricular function and reverse cardiac remodelling, in patients with dilated cardiomyopathy (DCM).[1] However, the cellular mechanisms by which β-blockers exert these beneficial effects in heart failure are not fully elucidated. Both Lowes *et al.*[2] and Yasumura *et al.*[3] showed that the functional improvement in DCM by the β-blocker treatment was related to normalization of the expression of genes that regulate contractile function, increases in sarcoplasmic-reticulum calcium ATPase and α-myosin heavy chain, and decrease in β-myosin heavy chain of myocytes. The myocardial extracellular matrix, composed of a complex network of structural proteins, mainly collagen Type I (Col I) and Type III (Col III), provides architectural support for the cardiac myocytes and plays an important role in myocardial contractile function[4] and cardiac remodelling.[5] Therefore, β-blockers are expected to normalize the collagen metabolism in the process of cardiac reverse remodelling.

Hormonal factors, such as angiotensin II, transforming growth factor-β_1 (TGF-β_1), osteopontin, endothelin-1, and cathecolamines[6] promote collagen synthesis. In DCM patients, the increased expressions of genes for both Col I and Col III were associated with a trend of increased expression of TGF-β_1.[7] In several experimental models, an increase in TGF-β_1 messenger ribonucleic acid (mRNA) is reported to precede the increase in collagen mRNA, suggesting that TGF-β_1 mediates the profibrotic effects of angiotensin II.[7–9] A blockade of angiotensin II also prevents myocardial fibrosis along with the production of myocardial hepatocyte growth factor (HGF), suggesting that HGF may have a role in the prevention of myocardial injury as a result of angiotensin II blockade.[10] Besides the effects of angiotensin II, remodelling of cardiac extracellular matrix has been reported to occur during β-adrenergic stimulation. The continuous β-adrenergic stimulation by either isoproterenol[11] or norepinephrine,[12,13] increased the expression

* Corresponding author. Tel: +81 6 6833 5012; fax: +81 6 6872 7486.
E-mail address: kitakaze@hsp.ncvc.go.jp

of collagen mRNA in rat ventricles and the β-blockers are reported to reduce collagen deposition of infarcted rats[14] or rats with chronic pressure overload.[15]

The aim of this study is to examine (1) the factors for the expression of cardiac collagen mRNA and (2) the effects of β-blockers on this expression in patients with DCM.

Methods

Study protocol

Thirty four patients referred to the National Cardiovascular Center, Osaka, Japan, because of congestive heart failure and accepted to undergo cardiac catheterization for the diagnosis of DCM, were enrolled. Four patients complicated with obvious hypertension and three patients with suspected secondary DCM were excluded. Three patients who could not tolerate the target dose of β-blockers and seven patients who did not undergo the second cardiac catheterization were also excluded. Finally, 17 patients were included in this study. The average time after the onset of the symptom was 3.1 years (3 months to 6.5 years). After their functional classes being stabilized by conventional therapy (*Table 1*), at least 1 month elapsed after the acute exacerbation, they underwent cardiac catheterization and were diagnosed as DCM. DCM was diagnosed by the absence of significant coronary artery disease as determined by coronary angiography, the absence of specific heart muscle disease or active myocarditis as determined by endomyocardial biopsy, and the reduction of left ventricular ejection fraction (<40%). Patients with obvious systemic hypertension, diabetes mellitus, a history of excess alcohol consumption, prior myocardial infarction, valvular heart disease, thyroid dysfunction, or other systemic diseases were excluded from this study. Written informed consent was obtained from all patients participated in this study according to a protocol, which was in agreement with the Ethical Committee at our institution.

Before the administration of a β-blocker, the plasma concentration of brain natriuretic peptide (BNP) was measured, ^{123}I-metaiodobenzylguanidine (MIBG) imaging was performed to measure the activation state of cardiac sympathetic nerve activity,[16–18] and the gene expressions of right ventricular myocardial samples obtained by the endomyocardial biopsy were assessed by the real-time reverse transcription–polymerase chain reaction (RT-PCR). Both left ventricular end-diastolic volume and ejection fraction were determined by left ventriculography. After cardiac catheterization, the patients were administered either carvedilol (12 patients) or bisoprolol (five patients). Attending physicians administered the β-blocker to the patient, according to the standardized regimen of β-blocker therapy. The initial doses of carvedilol and bisoprolol were 2.5 mg bid and 0.625 mg bid, respectively. These doses were doubled weekly until target dose (20 mg bid of carvedilol and 5.0 mg bid of bisoprolol). Four months after the onset of the treatment, all patients were re-admitted to repeat all of the medical examination performed at baseline. Follow-up MIBG imaging could not be performed in two patients who refused it.

Sixteen out of 17 patients received angiotensin-converting enzyme (ACE)-inhibitor and one patient received angiotensin II receptor blocker (ARB). Enalapril of 2.5–10 mg, quinapril of 10 mg, and temocapril of 2 mg daily were administered in 14, one, and one patients, respectively. Losartan as ARB was used at a dosage of 25 mg daily in one patient.

Table 1 Patients' demographics and baseline characteristics

Number (*n*)	17
Age (years)	48 ± 11
Sex (male/female)	16/1
NYHA classes I/II/III	4/12/1
Non-IHD/IHD	17/0
Treatment	
Furosemide, *n*(%)	14(82)
Spironolactone, *n*(%)	9(53)
Digitalis, *n*(%)	9(53)
ACE inhibitor, *n*(%)	16(94)
ARB, *n*(%)	1(6)
Vasodilator, *n*(%)	1(6)
HR (beats/min)	75 ± 14
sBP (mmHg)	112 ± 12
EDVI (mL/m^2)	153 ± 32
LVEF (%)	21 ± 7
BNP (pg/mL)	165 ± 146

IHD, ischaemic heart disease; HR, heart rate; sBP, systolic blood pressure.

MIBG imaging

After an overnight fast, patients underwent cardiac MIBG imaging. Anterior planar and single photon emission computerized tomography images were acquired 15 min (early) and 180 min (delayed) after injection of 111 MBq of general MIBG. A scintillation camera (GCA 901A/HG, Toshiba, Tokyo, Japan) with a parallel-hole general purpose collimator (low energy, high resolution type) was used. The camera was interfaced to the digital data acquisition system (GMS 5500 UI, Toshiba). The energy window of ^{123}I was centred at 159 keV with a 20% window. Anterior planar images were acquired using 512 × 512 matrix format for 180 s. Single photon emission computerized tomography images were reconstructed from a total of 30 projection images over 180° in 6° increments with 30 s per view using 64 × 64 matrix format. Global cardiac MIBG uptake was determined by the heart-to-mediastinum (H/M) count ratio on the planar image in both early and delayed imaging. Cardiac washout rate (WR) of MIBG was also determined from the equation $\{([H] - [M])_{early} - ([H] - [M])_{delayed}\}/\{([H] - [M])_{early}\} \times 100\%$, 16–18 as an index of cardiac sympathetic nerve activity.

Extraction of total RNA and synthesis of cDNA

We obtained the myocardial samples by endomyocardial biopsy from right ventricle. All of the myocardial samples were immediately frozen in liquid nitrogen and then stored at −80°C until use. The samples were homogenized in 1.0 mL ISOGEN™ reagent (Nippon Gene, Tokyo, Japan), thoroughly mixed with 0.2 mL chloroform, and centrifuged at 15 000 *g* for 15 min at 4°C. The aqueous supernatant was transferred into a micro test tube, mixed with 0.6 mL isopropanol, and centrifuged at 15 000 *g* for 15 min at 4°C. The precipitated total RNA was rinsed with 70% ethanol, air-dried, and then resuspended in RNase-free water. About 2 μg total RNA was treated with DNase Free™ reagent (Ambion, Austin, TX, USA) for 60 min, and then reverse-transcribed with Superscript II™ (Invitrogen, Carlsbad, CA, USA) at 37°C for 60 min using random primers (TaKaRa, Tokyo, Japan). The integrity of each complementary deoxyribonucleic acid (cDNA) mixture was checked by polymerase chain reaction (PCR) for the cDNAs of glyceraldehyde 3-phosphate dehydrogenase (GAPDH) and dystrophin, using ExTaq (TaKaRa, Tokyo, Japan) and the following primer sets: 5′-ACCACAGTCCATG CCATCAC-3′/5′-TCCACCACCCTGTTGCTGTA-3′ and 5′-GTACAAGAGGC AGGCTGATG-3′/5′-CTGAGCTGGATCTGAGTTGG-3′, respectively.

Oligonucleotides of primers and probes

Published cDNA sequences for human ACE, angiotensinogen, angiotensin II Type 1 receptor, mineralcorticoid Type 1 receptor, TGF-β_1, HGF, and Col I and III were used for construction of the primer sets and TaqMan probes as described subsequently. By Primer Express™ software (Applied Biosystems, Foster, CA, USA), several